Universidade de Aveiro
2014

Departamento de Química

Carlos Miguel Nóbrega Mendonça

Interações entre líquidos iónicos e modelo de membrana celular

Interactions between Ionic Liquids and Cell Membrane Models

Universidade de Aveiro
2014

Departamento de Química

Carlos Miguel Nóbrega Mendonça

Interações entre líquidos iónicos e modelo de membrana celular

Interactions between Ionic Liquids and Cell Membrane Models

Dissertação apresentada à Universidade de Aveiro para cumprimento dos requisitos necessários à obtenção do grau de Mestre em Biotecnologia Molecular, realizada sob a orientação científica da Doutora Ana Margarida Madeira Viegas de Barros Timmons, Professora auxiliar do Departamento de Química da Universidade de Aveiro e co-orientação da Doutora Sónia Patrícia Marques Ventura, Estagiária de Pós – Doutoramento do Departamento de Química da Universidade de Aveiro.

o júri

presidente Prof. Doutor João Manuel da Costa e Araújo Pereira Coutinho
Professor Catedrático do Departamento de Química da Universidade de Aveiro

Prof. Doutora Ana Margarida Madeira Viegas de Barros Timmons
Professora auxiliar do Departamento de Química da Universidade de Aveiro

Prof. Doutor Eduardo Jorge Morilla Filipe
Professor auxiliar do Departamento de Engenharia Química do Instituto Superior Técnico

Acknowledgments I would like to thank my Doctor Sónia Ventura and Professor Doctor Ana Barros for presenting me an interesting master thesis topic. Furthermore, I am grateful for their support, useful comments and guidance, during the elaboration of the first stage of my thesis, especially to Sónia Ventura who provided me a great help, attention, dedication, motivation and contribution on this work, a huge thank to her.

Furthermore, a big thank to Prof. João A.P. Coutinho for receiving me in his extraordinary group PATh and, also for the time that he has dedicated to this work.

A special acknowledgment to Prof. Ana Barros, who is guiding me since 2011 and for her availability to consider my integration on her research group. Moreover, she is the main responsible for my development and increased knowledge, not only in the practical, but also from a theoretical point of view.

Moreover, to all the teachers and friends that helped me through my difficulties making possible the concretization of my principal goals and dreams, especially my friends Ee Zin, Dario Néves and Gil Carraco, as well as Professor Ana Xavier. To them sincere acknowledgment. Moreover, special acknowledgments to Tânia Sintra for her extraordinary support. She spent so much time discussing, encouraging during this work and helping me in the thesis development.

Last but not least, thanks to my family. They never fail, they are always present listening, and giving constructive suggestions during these last years, especially my brothers, my sister and, more than everything, my mum and grandmother, You are simply awesome!

palavras-chave Líquidos iónicos, Risco (eco)ecotoxicológico, Modelos de membrana cellular, Filmes de Langmuir, Mecanismo toxicológico

resumo

Este trabalho propõe o estudo das interações, ao nível molecular, entre diversos líquidos iónicos (ILs) e membranas celulares mediante a aplicação de modelos de membrana celular segundo a técnica de Langmuir Blodgett. Pretendemos estabelecer uma melhor compreensão sobre o papel fundamental das interações de ILs com as membranas celulares, em particular os ILs da família imidazólio e colina. Assim, propõe-se a avaliação do efeito da concentração, bem como dos comprimentos da cadeia alquílica de ILs da família imidazólio, na organização e estabilidade de monocamadas lipídicas e a comparação com o comportamento de líquidos iónicos da família das Colinas. Em suma, este trabalho pretende fornecer uma visão sobre os factores moleculares que contribuem para a toxicidade dos ILs, que possam ajudar no desenvolvimento de ILs menos tóxicos.

keywords

Ionic liquids, (Eco)toxicological risk profile, Membrane cell models, Langmuir Films, Mechanism of toxic action

abstract

This work proposes the study of the interactions, at a molecular level, between diverse ionic liquids (ILs) and the membrane cells, by applying membrane cell models, namely Langmuir-Blodgett technique. We intend to establish a better understanding about the role of the interactions of ILs with membrane cells, in specific, the imidazolium and choliniumcholinium families. Hence, we propose the evaluation of the effect of the concentration as well as of the alkyl chain lengths of imidazolium ILs, on the lipid monolayers organization and stability and compare it with the behaviour of choliniumcholinium ILs. Summing up, this work is expected to provide an insight into the molecular mechanism contributing to the IL toxic activity that should help in the design of less toxic ILs.

Index

Figure index

Abbreviations and symbols

A– Molecular area

[Chol]Cl - Cholinium chloride

Cs^{-1}- Compressional modulus

Cs^{-1}-A - Compressional modulus as a function of the molecular area

Cs^{-1}- π - Compressional modulus as a function of the surface pressure

[C_2mim]Cl - 1-ethyl-3-methylimidazolium chloride

[C_4mim]Cl - 1-butyl-3-methylimidazolium chloride

[C_6mim]Cl - 1-hexyl-3-methylimidazoliumchloride

[C_8mim]Cl - 1-methyl- 3-octylimidazolium chloride

[C_{10}mim]Cl - 1-decyl-3-methylimidazolium chloride

DPPC - 1,2-Dipalmitoyl-sn-glycero-3-phosphocholinium

ILs - Ionic liquids

G – Gas phase

LE - Liquid-expanded phase

LE-LC - Liquid-expanded/liquid-condensed phase transition

LC -Liquid-condensed phase

RTILs - Room temperature ionic liquids

π – Surface pressure

π-A isotherm - Surface pressure- molecular area isotherm

π_c – Colapse pressure

1 – Introduction

1.1 – Ionic Liquids: Properties and applications

In the last decades, a new class of chemical compounds called room temperature ionic liquids (RTILs or simply ILs) have been developed. These chemical compounds are based exclusively on ionic systems, being liquids at room temperature. **(Plechkova N. and Seddon K., 2008)** Contrary to the molten salts which are produced by heating metallic salts at elevated temperatures (*e.g.* NaCl to over 800°C), ILs melt at temperatures below 100 °C **(Huddleston J. and Rogers R., 1998)** This new class of ionic compounds is constituted by a wide range of organic cations and inorganic or organic anions **(Brennecke J. and Maginn E., 2001)**. The most commonly ILs used to date are composed by cations such as imidazolium, pyridinium, pyrrolidium, piperidinium, quaternary ammonium, phosphonium, and cholinium plus diverse anionssuch as halide [Cl^-, Br^-, I^-], nitrate [NO_3^-], acetate [$CHCO_2^-$], trifluoroacetate [$CF_3CO_2^-$], tetrafluoroborate [BF_4^-], triflate [$CF_3SO_3^-$], hexafluorophosphate [PF_6^-], and bis(trifluoromethylsulfonyl) imide [$(CF_3SO_2)_2N^-$] **(Peric B. et al., 2012)**.(Figure 1)

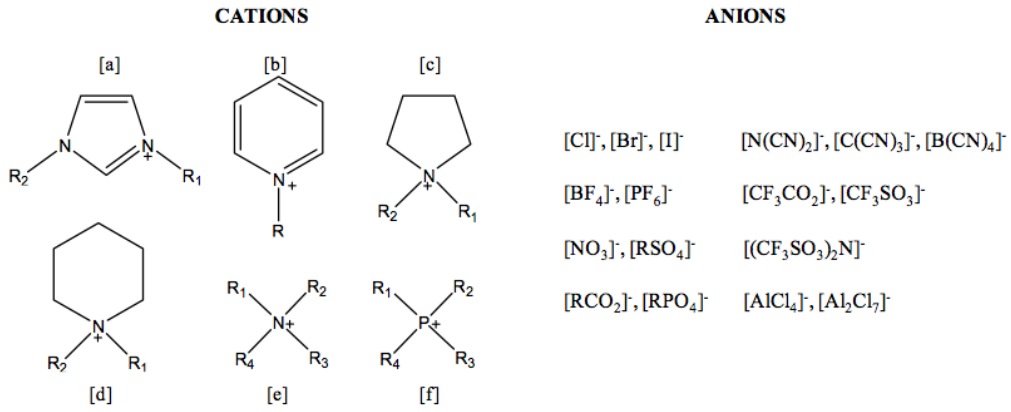

Figure 1: Principal ions used in the ILs synthesis. **(Peric B. et al., 2012)**

The combination of different ion types and the manipulation of the ions composition yield different ILs with unique properties, such as a wide liquid temperature range and high chemical and electrochemical stabilities **(Zhang S. et al., 2008)**. Low vapour pressures, non-flammability and thermal stability have gained much attention in the last decades, but it is the possibility of designing ILs with a specific set of properties to a certain scientific and industrial application that is calling the attention of the researchers. There is a huge expectation that from the research and the development of processes based in different ILs, real benefits in the technology field will arise. Moreover, ILs have

been cited as a promising tool to apply in the green chemistry field, due to their huge potential as alternative solvents for industrial catalytic reactions. **(Seddon K., 1997; Zhao D., 2002;Bourbigou H. and Magna L., 2002; Sheldon R., 2001)** Furthermore, their set of unique properties allows them to be used over a much wider set of applications, namely coordination chemistry **(Cocalia V. et al., 2006)** analytical chemistry **(Koel M., 2005)** polymer materials **(Kubisa P., 2005)** and nanotechnology **(Antonietti M. et al., 2004)**. Taking into account the unique properties and characteristics of ILs, diverse studies have been developed considering the implementation of these compounds in the development and optimization of a wide range of manufacturing processes, aiming at the reduction of their environmental impact and improving their economic viability. **(Plechkova N. and Seddon K., 2008; Anastas P. and Eghbali N. 2010)**

1.2 - Environmental assessment

The reduction of hazard potentials associated with the design, manufacture and use of chemical substances is one of the principal aims of Green Chemistry. **(Wasserscheid P. and Welton T. 2008;Anastas P. and EghbaliN. 2010)** Therefore, governments, industry and independent laboratories are joining efforts in order to develop methods to evaluate and to identify the potential hazards of new and existing chemical substances, aiming to reduce their environmental impact. **(Anastas P. and Eghbali N. 2010)** In order to protect human health and the environment, as well as concurrently maintain the competitive edge enhancing the capability of the EU chemicals industry, EU proposed a new regulation framework for the Registration, Evaluation, Authorization, and Restriction of Chemical Substances (the so-called REACH). **(Regulation E., 1999)** REACH regulates the safety of chemical products, their manufacturing process, toxicity, biodegradability, transport and use in the industrial sector. According to REACH regulation, the implementation and use of new chemicals requires a detailed (eco)toxicological evaluation. Therefore, ILs as new chemical products have to fulfil the requirement of REACH criteria before they can be commercialized. Although there were many reports emphasizing the attractiveness of ILs as green solvents due to their advantageous physicochemical attributes **(Welton T., 1999; Wasserscheid P. et al., 2008; Prasad A. et al., 2005)**, their sustainability, chemical risk and environmental impact should not be ignored. ILs are categorised as non-volatile substances, hence they are not considered as air pollutants. However, many ILs are soluble in water **(Freire M. et al., 2007),** which may cause water and soil contamination if accidentally released into

terrestrial and aquatic environment. Furthermore, recent findings showed that some imidazolium ILs were resistant to photodegradation **(Stepnowski P. and Zalesk A., 2005)** and scarcely biodegradable **(Gathergood N. et al., 2004; Garcia M. et al., 2005)**, which indicate that their effluents may accumulate in the environment. In this sense, REACH requested the examination of ILs' ecotoxicity, bioaccumulation, biodegradability, as well as its environmental fate, highlighting that ILs must be compliant under their criteria. **(Peric B. et al., 2012)** The first studies on ecotoxicity profile of the most used ILs on living organisms have been implemented based on numerous standard tests (OECD). These represent a flexible ecotoxicological test battery in the evaluation of ecological risk of ILs considering aquatic and terrestrial compartments, as well as different trophic levels, including the luminescent marine bacteria, freshwater green algae, crustacean, zebrafish as well as enzymes (for example the acetilcholiniumsterase from the nervous system) - Figure 2. Considering the aquatic environment, it is highly recommended the use of bioassays on standard test organisms as the cladoceran *Daphnia magna* (invertebrates) by **OECD (2008)**, the green alga *Pseudokircheriella subcapitata* by **OECD (2011)**, and the fish, *Danio rerio* (vertebrates) **(Pretti C. et al., 2009)**. However, a wide range of other tests using other organisms is also being investigated, namely the Growth inhibition test with *Lemna sp.* by **OECD (2006)** and the Acute Immobilisation test with *Daphnia sp*. by **OECD (2004)** In addition, some toxicity information on common ILs using the Microtox® assays **(Jennings V. et al, 2001)** was also considered.

Figure 2: Different aquatic organisms contemplated in the principal toxicological tests.

The Microtox® bioassay is a standardised toxicity test system, which is fast, sensitive, reproducible, simple and cost-effective. It is based on the bioluminescence inhibition assessing on the marine bacteria *Vibrio fischeri* when exposed to a

concentration range of a certain tested chemical. This toxicity test system is approved as a standard test to chemical toxicity on aquatic environments. **(Steinberg S. et al., 1995)** The end point of this methodology, EC_{50}, is used as a parameter to measure the concentrations of compounds in which 50% of the light emission from a specific strain of luminescent bacteria is reduced. **(Ventura S. et al., 2011)**

1.3 - Ecotoxicological risk profile

Although the ILs are frequently reported as an alternative solvent due to their negligible vapour pressure, similarities on the toxicological effects of some ILs have been shown to those observed for specific conventional solvents. Bernot and co-workers **(Bernot R. et al., 2005)** revealed on their studies that imidazolium-based ILs were more toxic to *Daphnia magna* than benzene, tri-cholоromethane and tetra-chloromethane. Cho and co-authors **(Cho C. et al., 2007)** have conducted a study on the use of several ILs and traditional organic solvents on the growth of the green microalga *Selenastrum capricornutum.* The authors observed that the ILs investigated were generally found to be two to four orders of magnitude more toxic than organic solvents such as methanol, dimethylformamide and 2-propanol. Based on these results, we may conclude that not all ILs are suitable as alternative solvents, but also that more studies are needed before their implementation in the industry. Other studies have been demonstrated that many of the common ILs used have different levels of toxicity for different living organisms **(Latala A. et al., 2005)**, **(Pretti C. et al., 2006).** These findings suggested that the toxicity of ILs could admit different levels of tolerance for different groups of organisms. The findings by Ventura and co-authors **(Ventura S. et al, 2011)** show that this tolerance could be related with variations on the morphological aspects of the external structure of the organism cell, since the morphological characteristics and chemical composition of the ultrastructure could be responsible for the protection of the microorganisms against the ILs "attack" **(Ventura S. et al, 2011)**. The mentioned results evidenced a wide range of coherent toxicological tendencies, that as the observations of many other researchers have been leading to a evaluation of different sources of toxicity of the ILs' structure, such as the alkyl chain length **(Garcia M. et al., 2005)**, the cation **(Couling J. et al., 2006)** and the anion **(Ranke J. et al., 2004; Garcia M. et al., 2005)**. Despite the general guidelines established about the toxicological potential of the most common ILs, few conclusions are known about the toxicological profile of some specific ILs families and chemical structures. Several studies have been done to identify the most important structural features that

affect the toxicity of ILs, being discussed that the toxicity of the ILs strongly depends of the cation or the alkyl side chain **(Ventura S. et al., 2012 a/b; Matzke M. et al., 2010; Pham T. et al., 2009).** In what concerns the toxicological profile of the cation, reports show that the aromatic cations like imidazolium and pyridinium are, in general, more toxic than non-aromatic ILs such pyrrolidium, piperidinium, ammonium and phosphonium **(Couling J. et al., 2006; Luis P. et al., 2007; Stolte S. et al., 2007; Pretti C. et al., 2009)** Based on those tendencies, Ventura and co-workers **(Ventura S. et al., 2013)**, have established in a recent study that the toxicity character of the cations can be divided into two main groups, the aromatic and non-aromatic ILs. In general, the toxicity observed for the aromatic cations seems to be related to the number of carbon atoms in the aromatic ring **(Couling J. et al., 2006)**. The evaluation of the relationship between structure and activity of ILs has been recently used to evaluate the toxicological effect of the cation alkyl chain length **(Garcia M. et al., 2005)**. These evaluations suggest that the magnitude of the ILs toxicity depends on the cation side chain length and that there is higher toxicity levels with the increase of side chain length (the so-called "side chain effect") **(Matzke M. et al., 2007/2010; Bernot R. et al. 2005; Cho C. et al., 2007; Ventura S. et al 2012-a)**. These results can be explained through the possible interaction of the alkyl chain of the cation with the cell membrane, which could disturb the interactions between the phospholipids, change the structure of the membrane and lead to loss of membrane stability and function **(Sikkema J. et al, 1995)**. The ability of an IL to interact with the cell membrane is usually associated with the lipophilicity nature of the cation **(Stepnowski P. and Storoniak, P. 2005; Ranke J. et al., 2007)**. This attribute was found to increase with the hydrophobic nature of the cation, which is related with the increase of the alkyl length **(Stepnowski P. and Storoniak P., 2005; Ranke J. et al., 2007)**. Literature results suggest that the lipophilicity is a key parameter on the toxicity of the ILs and that the analysis of lipophilic nature of the ionic liquids provides a better understanding of their adverse potential to organisms **(Stepnowski P. and Storoniak P. 2005).** However**,** the evaluation of the lipophilicity is not enough for the full understanding of the ILs toxicity, since the correlation between the increase in both the alkyl side chain length and toxicity is not linear for an indefinite alkyl chain length due to the "cut-off" effect **(Ventura S. et al., 2012 a/b; Matzke M. et al., 2010)** Various explanations are proposed for this phenomenon based either on insufficient solubility or kinetic aspects **(Matzke M. et al., 2010)**. The correlation between both lipophilic and hydrophilic nature of chemical compounds, with their biological activity has been widely used for assessing the toxicity of substances as well as used in modelling of environmental fate of organic chemicals. **(Hansch C. et. al, 1979)** Moreover,

chemical partitions have been used in several studies as a mechanism to evaluate qualitatively the capability of ILs to interact with cell tissues. **(Ventura S. et. al, 2011)** Toxicity tests for imidazolium- and pyridinium-based ILs carried out by Docherty and Kulpa **(Docherty K. et al., 2005)** confirm that the hydrophobicity of ILs induces an increase of the toxicity, which is in close agreement with literature **(Matzke M. et al., 2007; Ranke J. et al., 2004)**. Although the hydrophobicity of the alkyl chain can often be correlated with the lipophilicity parameter, the idea that high hydrophobicity corresponds to high lipophilicity is not always observed **(Matzke M. et al., 2007; Stolte S. et al., 2007)**. These results have improved the molecular understanding of some physicochemical properties of ILs, helping in the correlation of ILs parameters such as lipophilicity, hydrophobicity and bioaccumulation. It is expected that more hydrophobic compounds will show a lower solubility for water (Figure 3).

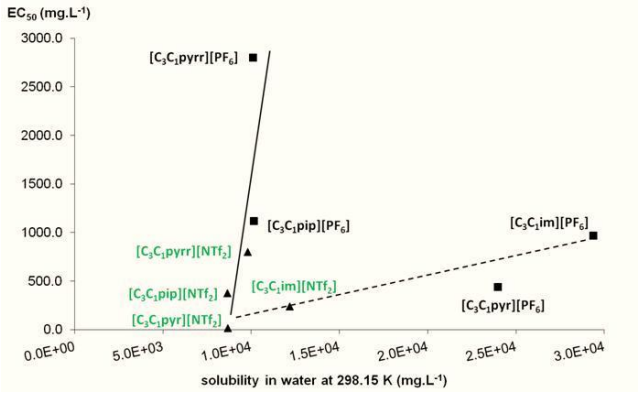

Figure 3. Relation between the water solubility of the different (aromatic and non-aromatic) ILs and their toxicity parameters (EC_{50} values) obtained by Microtox® assays. The lines in the figure are only for eye guide. This figure was adapted from literature **(Ventura S. et al., 2013)**.

Generally, a lower solubility in water would entail a higher affinity for the 1-octanol (solvent used in the octanol-water partition coefficient measurements which is an indirect via for the bioaccumulation assessment), which implies a greater ILs adherence to the living tissues that result in a higher toxicity and a lower EC_{50} value **(Ventura S. et al., 2011)**. Once there is a basic understanding of some of the relationships between the ILs toxicity and the nature of the alkyl chain, it starts to be clear that it should be possible to design less toxic ILs, based on short functionalised side chains. New researches aiming the design of less toxic ILs have been taking place through the incorporation of oxygenated groups into the alkyl chain **(Couling D. et al., 2006; Kumar R. et al., 2009; Ventura S. et al., 2013)**. Literature results show that functional groups such as ether, ester and hydroxyl within the side chains exhibited low toxicity compared to those with "simple"

alkyl side chains **(Kumar R. et al., 2009; Pham T. et al., 2009).** Those functional groups showed the ability to reduce the lipophilic nature of the alkyl chain, which might reduce the ability of ILs' to interact with the cell membrane and consequently reduce their toxicity **(Stolte S. et al., 2007; Ventura S. et al, 2012-b)**. However, different effects are found for different functional groups meaning that more investigation is needed in order to select the less toxic and task-specific functional groups.

The contributions of the anion moiety for the ILs toxicity are still insufficiently understood as little information and data are known about their *in vivo* and *in vitro* behaviour. Initially, several researchers have reported that no general influences were found for the anion part of the IL in their toxicity and consequently, that the anion effects were less significant compared to the side chain effects of the cation **(Ranke J. et al., 2004; Garcia M. et al., 2005; Bernot R. et al., 2005)** In contrast, additional studies clearly demonstrated that the type of anion can strongly affect the toxicity of the IL, and that some seem to have a higher toxicity than others **(Frade R. et al., 2007/2009)**. For example, toxicity tests using different anions showed that the hydrophobic bis(trifluoromethylsulfonyl)imide $[NTf_2]^-$ anion is able to decrease the toxicity of several ILs, independently of the cations tested **(Frade R. et al., 2007; Kumar R. et al., 2009; Stolte S. et al., 2006)**. In contrast, the toxicity observed for guanidinium-based ILs increased when combined with the anion $[PF_6]^-$, comparatively to $[NTf_2]^-$ and dicyanamide $[N(CN)_2]^-$ **(Frade R. et al., 2007)**. Based on the entire set of studies reported in literature, it is possible to postulate that the toxicity of hydrophobic anions has a much bigger effect for shorter alkyl chains and less toxic cation **(Kumar R. et al., 2009; Stolte S. et al., 2006)**.

Interestingly, and although the (eco)toxicological effect of ILs has been widely studied and characterized by a diversity techniques, just a few studies have been performed considering the cell membrane as the principal subject. Thus, the study of the interactions between membrane cell and ILs is scarce and underexplored. In a recent work, where different ILs were applied as impregnation reagents to provide the higher conductivity to SEM biological samples, some distinct phenomenological changes on the cellular membrane of the biological material used appeared **(Kawai K. et al, 2011).** Imidazolium and cholinium-based ILs were applied in this study, the results showing that while the imidazolium cation induced the appearance of rugged surfaces with deep wickless, the biological matrices impregnated with the cholinium presented smooth surfaces without deep hollows **(Kawai K. et al, 2011)** (Figure 4).

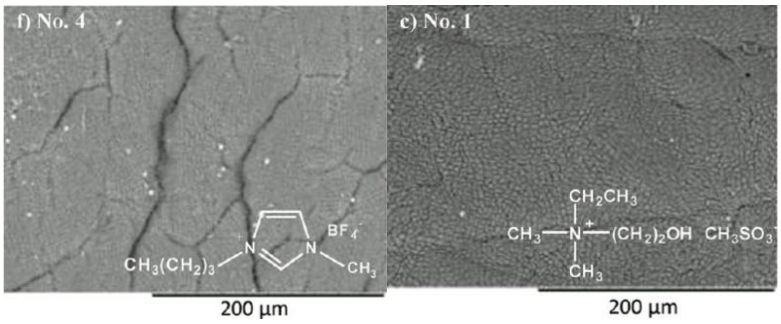

Figure 4: SEM images of Seaweed surfaces impregnated with ILs. **(Kawai K. et al, 2011)**

Comparing the results, it was possible to establish that the imidazolium family, showed a slow penetration but a higher level of damage on the cell membrane. This result was expectable due to the octanol-water partition coefficients of the imidazolium ionic species reported so far that suggest that this IL cation has a higher ability to interact or to accumulated in the cell membranes. Meanwhile, the cholinium family was capable of penetrate through cell membranes, but without dissolution or changing the original shape of the biological samples.

On this work we propose the study of the mechanism of action of the imidazolium and cholinium based ionic liquids upon biological membranes. We propose the use of Langmuir Blodgett technique as simple and sensitive tool to evaluate the phenomenon involved on the interaction of these two ionic liquids families. Summing up, we intend to explore theoretically and practically some of the hypotheses involving the structure parameters of both ILs and the toxicological effect that have been pointed has hazard on the various toxicity tests reported so far **(Matzke M. et al. 2010; Ventura S. et al., 2013)**.

1.4 – Cellular membrane

The cellular membranes are dynamic structures responsible for the demarcation of the border between the intra-and extracellular medium of the cells. It consists of a fluid bilayer of approximately 7-10 nm thickness, mainly composed by lipids, proteins, sterols and some polysaccharides. The membrane lipids comprise an extensive variety of amphipatic compounds with a nonpolar (alkyl chain) and a polar region. In animal cells, the lipids presented in greater quantities are phospholipids, followed by sphingolipids, which also appear in significant quantities. Various phospholipids can be distributed preferentially in the outer membrane sheet, such as derivatives of phosphatidylcholine (PC) and sphingomyelin, or preferentially in the interne leaf, such as derivatives of phosphatidylethanolamine (PE) and phosphatidylserine (PS).

1.5- Major Model Membrane Systems

Since the biological membranes are very complex systems, several models aiming at mimicking of the biological membranes have been developed **(Singer J. et al, 1972; Vestergaard M. et al, 2008)**. These models have been used as simple approaches to the study of membrane structure, properties and processes **(Thakur G. et al, 2009)**. As they can be performed under controlled conditions, providing advantages to live cells approaches, they can be applied in diverse perspectives, **(Matsuzaki K. et al., 2007; Planque M. et al., 2007; Devanathan S. et al., 2006; Verdier Y. et al., 2004; Paun G. and Rozenberg G. 2002; Khan M. et al, 2013)** including toxicology **(Torrano A. et al., 2013).** These studies have increased our understanding about membrane function and structure, providing important information for the development and progress of a wide range of scientific and technological areas. The best-known and more common model membrane systems used are lipid vesicles, supported lipid monolayers/bilayers and lipid monolayers **(Eeman M. and Deleu M., 2009)**.

1.5.1- Lipid vesicle models

The lipid vesicle models are commonly applied to study the membrane phase behaviour as well as to investigate membrane process such as membrane fusion, molecular recognition and cell adhesion **(Vestergaard M. et al., 2008)**. These structures are versatile biomimetic model membranes, which display a concentric lipid bilayer with variable size range, obtained by aqueous dispersions of membrane lipids **(Eeman M. and Deleu M., 2009)**. The first work on the study of membrane interaction of ILs using vesicles systems has been report by Gal and co-workers **(Gal N. et al., 2012)**. In a quest to understand the role of the ILs molecular parameters on their biological activities, the researchers evaluated the interactions between representative ILs, exhibiting distinct structural and biological features, and lipid/polydiacetylene (PDA) vesicles. The study provided a biophysical and microscopy analysis on the effect of ILs upon the lipid bilayer insertion, surface interaction, lipid reorganization and membrane disruption. It has been possible to observe that the ILs exhibit different membrane binding, insertion and disruption mechanisms depending to their structure, and that the increase in the membrane activity followed the increase of the cation side chain length of the ILs. The authors suggest that the vesicles membranes might be affected by electrostatic

interactions between the cation moieties and the negatively charged lipids and that this effect could be one of the mechanisms of action of IL on the real cell membrane due to the fact that most cellular membranes exhibit charged molecules at the surface.

1.5.2 - Supported lipid monolayer/bilayer models

The supported lipid monolayer/bilayer models are lipid structures confined to a solid surface, usually mica or silica. **(Peetla C. et al., 2009)** These biomimetic models are generally formed by transference of monolayers spread at the air-water interface **(Clausell A. et al., 2004; Ihalainen P. et al., 2002),** or by "fusion" of lipid vesicles onto a smooth and solid surface **(Mingeot-Leclercq M. et al., 2008).** The use of these model membrane lies on the characterization of the structure and morphology of the membrane surface following the interaction with specific molecules. In a recent study Massimiliano and co-workers **(Galluzzi M. et al, 2013)** have introduced the first experimental report of the ILs interaction with supported lipid models. The authors studied the effects of the different anions and cation lateral side chain length of imidazolium ILs on DOPC phospholipid monolayers. The results suggest the existence of interactions between the imidazolium-based ILs and DOPC phospholipid monolayers, being these interactions associated with the length of side chain on the cation, but not significantly associated with the anion nature. The results showed the importance of the hydrophobic/lipophilic character of the ILs cations, since short (C2 and C4) lateral chains adsorb reversely on the phospholipid monolayer, and long chains (C8 and C12) promote a stronger irreversible interaction. The authors also report that the ionic liquids were able to replace the DOPC coated on the surface of the electrode, which can constitute one determinant effect on the cell membrane stability.

1.5.3 - Lipid monolayers models

The lipid monolayers models, also referred as Langmuir films, are monomolecular insoluble monolayers formed on the surface of the water by amphiphilic molecules **(Brockman H., 1999).** These biometric models display a well-defined and stable structure, possessing a homogenous bidimensional system with a planar geometry **(Eeman M. and Deleu M., 2009)**. The Langmuir films are a simple and effective system as well as stable, rapid and relatively inexpensive predictive technique. Studies using Langmuir monolayers at the air-water interface have been taking place as a successfully

and simple model to elucidate the surface behavior of cell membranes **(Leblanc R., 2006).** These studies have reported interesting phenomena that are providing a better understanding of the interaction between different classes of molecules with the cell membrane in a biological environment. However, no study has yet been performed applying the principles of Langmuir films on the study of ILs toxicity.

1.5.4 -Langmuir and Langmuir-Blodgett Technique

The amphiphilic nature of surfactants and their high surface activity at the air-water interface allow them to be spread onto a polar liquid surface **(Schwartz D. et al., 1997).** Sweeping these molecules over the liquid surface makes possible their compression into an ultra-thin ordered monomolecular layer **(Kaganer V. et al., 1999).** These films behave as an elastic membrane trapped at the air-water interface that can be repeatedly compressed and expanded**.** Monolayers obtained by this methodology are known as Langmuir films, and for experiments performed with phospholipids, the film resembles half of a phospholipid bilayer **(Schwartz D. et al., 1997).** The typical procedure used in the fabrication of Langmuir monolayers consists in the spread of a specific volume of a suitable volatile organic solvent, with a known amount of amphiphilic molecules, at the surface of an aqueous interface **(Orbulescu J. et al, 2009).** The spreading solution is applied uniformly on the aqueous surface under a dropwise process. After solvent evaporation, the Langmuir film forming material attains their favored configuration at the air-water interface **(Orbulescu J. et al, 2009).** The molecules are organized with their hydrophobic hydrocarbon chains ("tails") oriented towards the gas phase and the hydrophilic polar group ("head") immersed in the aqueous phase **(Kaganer V. et al., 1999).** By compression of the molecules at the air-water interface a floating monolayer is formed **(Iwamoto M. et al, 1996).** The transfer of this Langmuir monolayer onto a solid substrate lifting vertically one solid substrate immersed in the subphase, allow us to prepare one Langmuir-Blogett film **(Petty M., 1996; Schwartz D. et al., 1997).** One or more layers can be transferred on the preparation of Langmuir-Blodgett films depending of the number of passages made by the substrate through the water surface. For an easier cleaning and a higher accuracy, the Langmuir films are usually produced in a container known as trough. This trough is coated by a hydrophobic and inert material (Teflon) and it contains the subphase. In addition, the trough comprises one thermostatic water channel system that ensures a constant temperature throughout the entire experiment. One or more movable Teflon barriers are placed across the trough to allow the compression of

the monolayer formed on the surface. One surface pressure sensor is connected to measure the surface tension variation of the air-water interface along the compression and decompression process, and a device named dipper is used on the deposition of monolayers onto solid substrates **(Dynarowicz-Łątka P. et al., 2001; Schwartz D. et al., 1997)** - Figure 5.

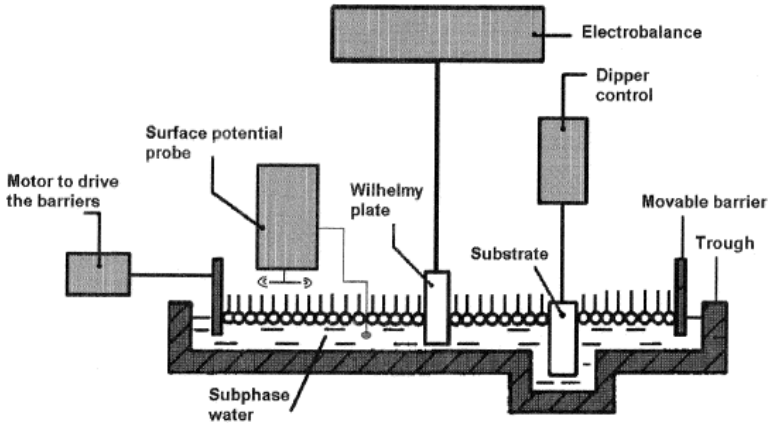

Figure 5: Representation of a typical Langmuir Trough.(**Dynarowicz-Łątka, P. et al., 2001**)

The nature of the surface-active molecules at the surface of the water favors the decrease of the surface tension. Measuring the variation of the surface tension during the film compression the behavior of a monolayer can be studied. The difference between the surface tension of pure and clean water and surfactant-covered water is known as surface pressure and it is expressed by Equation 1. **(Hann R. and Kathirgamanathan P., 1990)**

$$\pi = \gamma' - \gamma \qquad \textbf{Equation 1}$$

Where, **π** is the surface pressure of the water, **γ'** represents the surface tension of pure and clean water (72.7 $mN.m^{-1}$ to pure water at 20 ºC) and **γ** the surface tension of the water covered with the surfactant. Since the number of molecules spread on the subphase surface is known, it is possible to measure the surface pressure as a function of the area occupied *per* molecule **(Schwartz D. et al., 1997; Petty M., 1996)**. The measurements of the surface pressure are commonly carried out using a Wilhelmy plate attached to a microbalance. The Wilhelmy plate is partially immersed in the subphase, and allows the construction of a pressure-area isotherm **(Kaganer, V. et al., 1999; Orbulescu, J. et al, 2009**).

1.5.5 - Analysis of Stearic Acid (SA) isotherm

The stearic acid (SA), a "classical" surface-active material, is frequently used in the standardization of Langmuir film studies due to their simplicity and well-defined properties at the air-water interface **(Hann R. and Kathirgamanathan P., 1990)**. By monitoring the changes in the surface pressure during the compression of a stearic acid monolayer, a pressure-area isotherm is constructed (Figure 6).

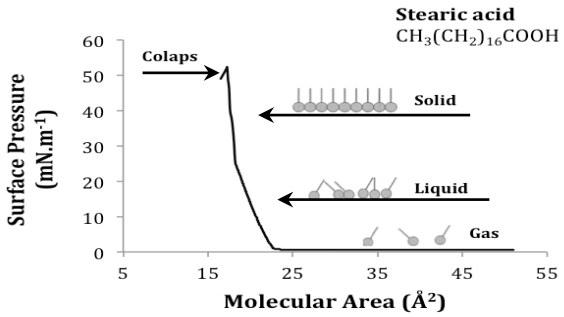

Figure 6: An idealized stearic acid isotherm showing the molecular orientations.

The isotherm shows tree distinct packaging phases used on the interpretation of the organization, dynamics and molecular stability of the SA Langmuir film. After the initial deposition of molecules on the subphase, without any external pressure applied to the monolayer, the molecules act as a two-dimensional gas **(Dynarowicz-Łątka P. et al., 2001; Kaganer V. et al., 1999**). In this phase, the molecules are randomly distributed throughout the air-water interface without a specific order. This phase is characterized and classified by the absence of interactions between the organic molecules and the subphase itself, which corresponds to a surface pressure equal to zero **(Kaganer V. et al., 1999**)**.** By compressing the film, the amphiphilic molecules start to interact with each other and with the subphase, acting as a two-dimensional liquid. At this stage, the molecules begin the formation of regular arrays and the film starts to achieve some order **(Kaganer V. et al., 1999**)**.** This phase is characterized by a decrease of area *per* molecule, increase of the hydrophobic tails interactions and consequent increase of the van der Waals interactions **(Dynarowicz-Łątka P. et al., 2001; Iwamoto M.et al, 1996).** Continuing to tighten the barriers, the area around each molecule reaches a minimum and the molecules form an ordered and compacted monomolecular film **(Crawford N. et al, 2013).** This stage is classified as the solid phase and it is characterized by a linear relationship between the surface pressure and the molecular area. **(Dynarowicz-Łątka P.**

et al., 2001; Kaganer V. et al., 1999). By further applying an external pressure, the molecules are expelled out of the monolayer plane, causing the film collapse and the loss of the ordered monomolecular structure. The pressure needed to promote the film collapse is called collapse pressure (πc) and defines the maximum pressure that the monolayers can be compressed without losing their monomolecular structure **(Kaganer V. et al., 1999).** Quantitative data such as, the molecular dimensions and organization of the monolayer, can be obtained through the analysis of an isotherm. When the monolayers exist in the solid phase, the molecules arrangements are well organised and closely packed. The molecular area at zero pressure (A_0) can be determined by extrapolating the slope of the solid phase to zero pressure. The point where the line crosses the x-axis is the hypothetical area filled by one molecule in the condensed phase at zero pressure. Considering the SA as an example, it is possible to determine that the area filled by a SA molecule in a condensed phase at zero pressure is about 20 to 22 $Å^2$ **(Dynarowicz-Łątka P. et al., 2001).** The area obtained is reported as the cross sectional area of a hydrocarbon chain, which indicates that this compressed monolayer, has their hydrophobic chains oriented almost vertically **(Dynarowicz-Łątka P. et al., 2001).** Different strategies and complementary analysis techniques are nowadays available for a more complete and strict interpretation/understanding of the properties of the Langmuir films, such as surface potential-area, electrical measurements, microscopic measurements, spectroscopic measurements, X-ray and neutron scattering measurements, non-linear optical measurements and other techniques as sum-frequency generation (SFG) spectroscopies **(Dynarowicz-Łątka P. et al., 2001).**

1.6 - Intermolecular interactions

The understanding of intermolecular interactions is extremely important in order to understand the behaviour of the chemical and biological systems at molecular level. They are therefore, from the thermodynamic point of view, similar as it became obvious that the phenomena controlling these interactions are, in fact, based in the same basic thermodynamic principles. As discussed above, the Langmuir technique will be used in this work as a practical and simple methodology to provide a generic biophysical insight on some of the various molecular interactions acting between ILs and lipidic films.

1.7 – Interactions of biomolecules with Langmuir films

The advantage of using a model membrane is to prevent handling the abundance of factors, which may cause varied impacts on the active molecules/cell interface dynamic and make difficult the interpretation of the results. Therefore, by using Langmuir monolayers it is possible to resemble the first barrier met by an active molecule, which moves towards the cell membrane. Furthermore, this technique permits the analysis of specific molecular level interactions between the selected materials and the cell membrane components under controlled conditions. Two main objectives arise from the use of Langmuir films; i) the first associates the interactions at a molecular level with the physiological activity of different types of biomolecules; ii) the second combines results with toxicity data, based on the interaction between the chemicals and the cell membranes. In what concerns the study of the interaction between active molecules and the Langmuir films, a wide range of strategies have been developed in the last decades, usually depending on the experiment objective and the molecules under study. Important advances on the study of chemical and biological reactions of several biomolecules with monolayers serving as cell model were descrived. A relevant part of those works was performed involving studies of the chitosan interaction with the cell membrane **(Pavinatto F. et al., 2005)**. Pavinatto et al. concluded that the interactions acting between the chitosan and the cholesterol monolayers occur by specific groups of chitosan (-NH_3^+ and OH) and cholesterol (-OH), mainly by hydrogen bonds. These conclusions were also taken by Parra-Barraza and co-workers **(Parra-Barraza H. et al., 2005)** on the study of the interactions of SA and cholesterol Langmuir films for four different chitosans with distinct molecular weights. For the same concentration of chitosan in the subphase, significant modifications in the isotherms were found, meaning that distinct interactions between both components SA and cholesterol are occurring. In fact, based on theoretical calculations, the author demonstrated that the interactions between chitosan and the cholesterol were triggered by –NH_3^+ and –OH groups. On the other hand, the interactions between deprotonated SA were established mainly by electrostatic interactions between the groups –NH_3^+ and –COO^-. Based on observations of more complex studies with mixed films of cholesterol and phospholipid dimyristoyl phosphatidic acid (DMPA) conducted by Pavinatto and co-workers **(Pavinato F. et al., 2009)** the authors proposed a model for the interaction between chitosan and DMPA monolayers. The model assumes that the mechanism of action of chitosan starts by the migration from the subphase to the interface and subsequent interaction with the mixed monolayer, mainly by electrostatic forces.

Then, chitosan penetrates on the lipid monolayer inducing the expansion of the film and a conformational ordering of the hydrophobic chains. In additional studies, Silva and co-workers **(Silva C. et al., 2012)** examined the mechanism of action between chitosan and mixed films of DMPA and the protein mucin (one of the main components of the mucus). The surface pressure and surface potential isotherms were performed with DMPA monolayers onto which chitosan and/or mucin were adsorbed. The mucin was adsorbed on the DMPA monolayer, causing a large expansion in the isotherm and decreasing the surface elasticity, due to the higher affinity of mucin to biomembranes composed by negatively charged phospholipid molecules. The addition of chitosan in the subphase after the saturation of the mucin adsorption on the film resulted in the decrease of the expanding effect of mucin on the DMPA monolayer, which was a consequence of the formation of complexes between the mucin and the chitosan (promoted by electrostatic interactions). With the high potential and crescent applications of nanomaterials, major concerns about their toxicological and environmental effect have emerged. Early, studies have demonstrated a high capability of nanomaterials to establish interactions with cellular components and to penetrate into the cell membrane. **(Huang Z. et al., 2008; Cancino J. et al. 2011)** However, considering the complexity of the mechanisms involved in these interactions, a lack of knowledge between physicochemical and biological parameters of nanomaterials is still surprisingly high. Recently, researchers have been discovering on the Langmuir Blodgett technique an opportunity to obtain insights on some of the toxicological mechanisms of some nanomaterials. Guzman and co-authors **(Guzmán E. et al., 2013)** investigated the interaction effect and incorporation potential of silica nanoparticles, observing that the nanoparticles were incorporated into the lipid film through specific interactions between the nanoparticles and the lipid molecules. The study of the interactions of oppositely charged gold nanoparticles with cell membrane studied in detail by Torrano and co-workers **(Torrano A. et al., 2013),** found that the electrostatic forces are needed when nanoparticles interacted with model membranes, especially when negatively charged monolayers are considered. These effects might have important connections with the toxicity observed for these nanostructures, which relies heavily on the capability of guest substances to modify the elasticity of the membrane to promote mass transport through the membrane.

2 - Materials and methods

2.1 - Materials

The ILs studied were 1-ethyl-3-methylimidazolium chloride ([C_2mim]Cl), 1-butyl-3-methylimidazolium chloride ([C_4mim]Cl), 1-hexyl-3-methylimidazoliumchloride ([C_6mim]Cl), 1-methyl-3-octylimidazolium chloride ([C_8mim]Cl) and 1-decyl-3-methylimidazolium chloride ([C_{10}mim]Cl). All ILs were purchased from Iolitec (Ionic Liquid Technologies, Germany). The Cholinium chloride ([Chol]Cl) (98 wt%) was purchased from Sigma–Aldrich®. Ultrapure water, pH = 5,70 and resistivity 18,2 MΩcm, were provided by a Millipore purification system and used to prepare all IL's aqueous solutions.1,2-Dipalmitoyl-sn-glycero-3-phosphocholine (DPPC) (≥ 99%), was purchased from Sigma-Aldrich®. Chloroform, HPLC grade (99,9%), was acquired from Sigma-Aldrich.

2.2 -Metodology

Langmuir monolayers were prepared using a NIMA 611 Langmuir-Blodgett trough. Surface pressure-area (π-A) isotherms, isocycles and surface pressure-time curves were performed at room temperature and measured with a Wilhelmy plate balance. Typically monomolecular films were produced by spreading 60μL of a chloroform solution of the amphiphilic molecules (1 $mg.mL^{-1}$), using a microsyringe (Hamilton, 100μL), at the air-water interface. Langmuir monolayers were allowed to reach equilibrium for 10 min before compression. The compression rate applied to the pressure-area isotherm measurements was 10cm^2 min^{-1} (2.4 $Å^2$ min^{-1}). The influence of the different ILs in the subphase of the neutral/zwitterionic (DPPC) Langmuir monolayers was studied at several concentrations. These concentrations were obtained by diluting the ILs in ultra-pure water taking into consideration their water content. The isocycles were performed between a pressure of 0$mN.m^{-1}$ and 30$mN.m^{-1}$ approximately, and at a compression rate equal to 50$cm^2.min^{-1}$. This experimental procedure was repeated three times without any intervals between each cycle of compression/expansion. The adsorption measurements of the ILs were performed using distinct procedures: (i) motorization of the surface pressure variation at constant area as overtime in the absence of lipids on the interface; (ii) motorization of the surface pressure variation at constant area over time in the presence of lipids at the interface upon compression of the DPPC monolayer up to a surface pressure of 16 $mN.m^{-1}$; and (iii) motorization of the surface pressure variation at constant

area over time, via injection of an IL solution on the subphase, after compression of the DPPC monolayer up to a surface pressure of 16 $mN.m^{-1}$. Changes in the mechanical properties and DPPC monolayer were also studied through the calculation of the compressional modulus (Cs^{-1}), also known as in-plane elasticity, from the π-A isotherms data by applying Equation 2 **(J. T. Davies and E.K. Rideal, 1963)**:

$$Cs^{-1} = -A(\partial\pi / \partial A) \qquad \textbf{Equation 2}$$

Where Cs^{-1} is the surface compressibility modulus, A is the molecular area and π the surface pressure

3 - Results and discussion

The present study aims at the evaluation of the molecular interactions between the imidazolium ILs family and DPPC monolayers in order to obtain information that could provide a better understanding about the differences of their mechanism of toxic action. For comparison a cholinium was also studied. Monolayers at the air-water interface mimicking the cell membrane outer leaflet were formed by spreading a chloroform solution of the DPPC phospholipid onto a subphase containing the ILs. The interactions between the phospholipids and the ionic liquids were studied by film balance measurements followed by the analysis of the surface pressure-area isotherms and calculation of the monolayers compressibility modulus. The stability of the monolayers was also assessed via three consecutive compression-expansion cycles also referred as isocycles. Notice that the experiments were performed and the results interpreted taking as reference the values of EC_{50} of the [C_6mim]Cl and [Chol]Cl (170,0 and 469,3 mg/L to 30 min of exposure). As during the initial stages of the experimental work a number of inconsistencies were identified between replicates, several experiments were conducted and a significant number of publications on trends in the pressure-area isotherms reviewed in order to identify and correct these errors as discussed next.

3.1 – Experimental errors

In the first section of this work, some of the most critical sources of experimental error identified are defined and the strategies to minimize or correct them are presented and discussed.

3.1.1 – Over-flow/ film leakage phenomenon

During the compression of the monolayer at high surface pressures, it was observed that the subphase started to overflow the trough. The overflow process started near the barriers (Figure 7-a) and, as the superficial film was continuously being compressed, under the walls of the trough (Figure 7-b).

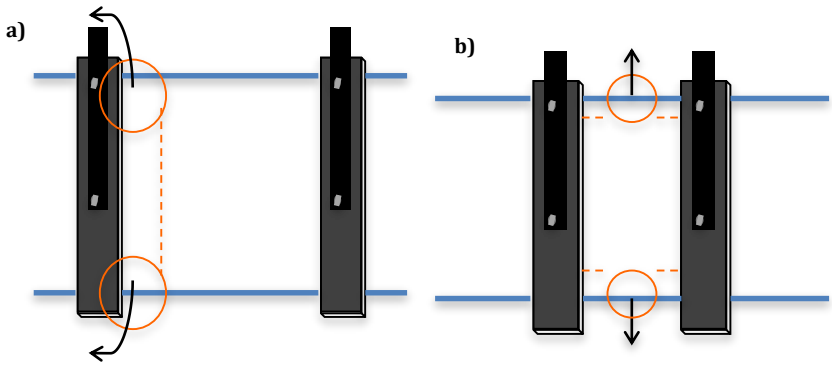

Figure 7: Representation of the over-flow phenomenon observed during the compression of the monolayer at high surface pressures**,** first near the barriers (a) and then under the walls of the trough (b).

Typically, as the overflow phenomenon evolves, the subphase level drops and film leakage occurs. Traditional measurements of the interfacial behavior of insoluble surfactants are extremely sensitive to this effect as it involves the loss of material from the air-water interface. Consequently, changes in the measurement of area *per* lipid occur, affecting the shape of the isotherm and leading to situations such as, the premature occurrence of the film collapse **(Tabak S. A. and Notter R. H., 1977)**. Like us, several researchers have been correlating the leakage effect with sources of experimental errors such as irreproducibility of the isotherms profile and shifts of the minimum area per molecule at LC phase, specially for films of high relatively rigidity and large dynamic collapse pressure such as DPPC **(Notter R. H. et al., 1980; Tabak S. A. et al., 1977)**. Figure 8 shows the effects of this phenomenon on the pressure-area isotherm of DPPC monolayers.

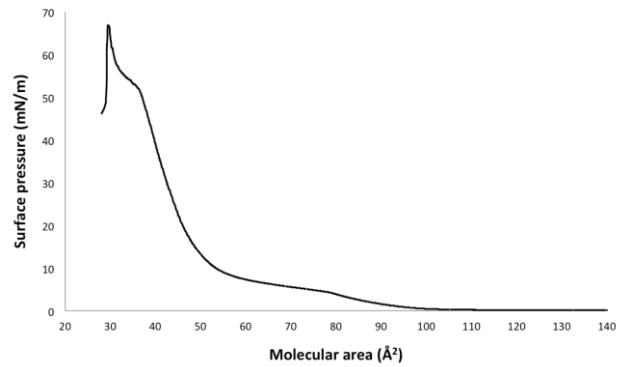

Figure 8: Effect of the subphase overflows and film leakage during the study of pressure-area isotherm of DPPC monolayers on pure water.

The first decrease in the slope of the pressure-area isotherms, observed at surface pressures at around 55 $mN.m^{-1}$, resulted from the film leakage near to the barriers. At this point, the losses of material are small which allow the self-reorganization of the film inside the trough and the continuous increase of the surface pressure. As the surface pressure reaches maximum values, the subphase overflow takes place at a much more significant level, and the irreversible and substantial loss of material causes subsequent and the accentuate decrease of the surface pressure. As the leakage effect involves different levels of material losses between assays, distinct collapse pressures are obtained, which lead to misinterpretation of the results. In one attempt to minimize the effects of film leakage, additional studies regarding the evaluation of the subphase volume influence on the overflow phenomenon were performed. Using different volumes of ultra pure water, it was possible to conclude that the potential of the subphase overflow and film leakage was higher when larger volumes of water were used. We observed that in these cases, the curvature angle of the water with respect to the barriers and the walls of the trough increased, affecting the dynamic collapse pressure of the monolayers. We believe that for high curvature angles, the DPPC phospholipids trapped in a transient or non-equilibrium state between the interface and the boundaries of the barriers during the compression increase (Figure 9).

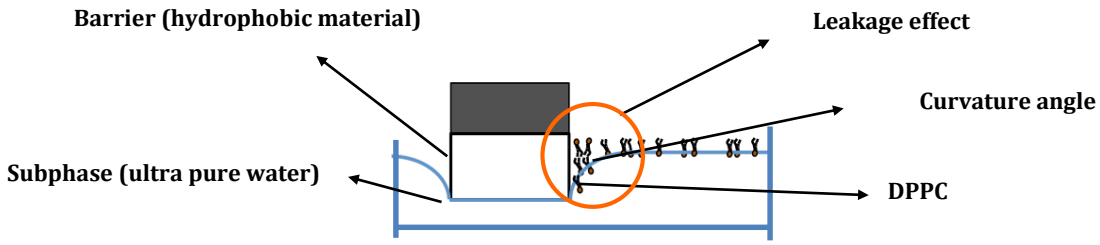

Figure 9: Representation of the curvature angle of the water with respect to the barriers for high volumes of subphase. The image show DPPC phospholipids trapped between the boundaries of the barrier and interface during the compression of a monolayer.

This increase, induces higher levels of disorder of the DPPC molecules at this specific region, contributing to the subphase overflow phenomena and consequently film leakage. Despite a significant decrease of overflow phenomenon with the decrease of subphase volume, phenomena associated with the hysteresis of the Wilhelmy plate contact angle occur during the assays performed with the lowest volumes tested. These phenomena involved the progressive decrease and subsequent loss of contact between the Wilhelmy plate and the interface during the compression of the film, which turned impossible the monitoring of the surface pressure until the end of the film compression (Figure 10).

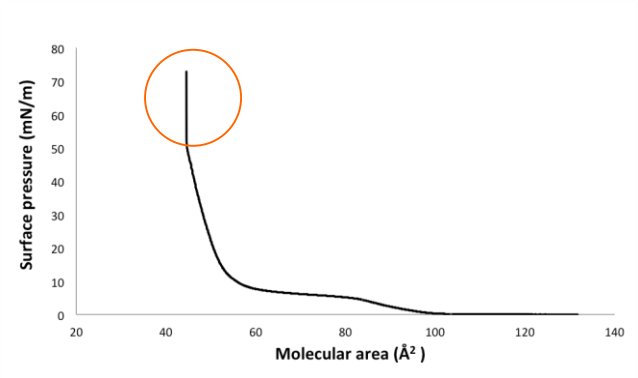

Figure 10: Consequence of the Wihelmy plate contact angle hysteresis on the study of the pressure-area isotherm of DPPC monolayers formed on ultra-pure water.

As Teflon has a hydrophobic nature and since the curvature angle effect is inherent to the barriers and walls, we were unable to completely avoid the overflow and leakage phenomenon. However, by reducing the subphase volume the problems associated with overflow and leakage were overcome. Based on our observations, it is possible to conclude that the volume at which the overflow remained at its minimum and at which there is no Wilhelmy plate contact angle hysteresis is 450 mL, which corresponds to a the level of the subphase that is slightly lower than the level of the trough walls but still within that of the barriers. Tabak and co-workers **(Tabak S. A. and Notter R. H., 1977; Tabak S. A. et al., 1977)** found that troughs equipped with a continuous Teflon ribbon barrier were able to avoid the film leakage when compared with standard barriers. The authors proved that the use of ribbon barriers instead of the conventional Teflon barriers enables a better confinement of the monolayer at higher packing densities (> 70mN.m^{-1} for DPPC). Thus, as the through used in this work is composed by a set of conventional Teflon barriers, it is expected the occurrence of experimental limitations in what concerns film leakage.

3.1.2 - Isotherm reproducibility

The shape of the isotherms is a critical parameter on the interpretation of the molecular thermodynamics and morphological properties of insoluble monolayers. Therefore, accurate measurements and high level of reproducibility are essential parameters for a proper analysis. Figure 11 shows some of the pressure-area isotherms obtained from the study of the DPPC monolayers in ultra-pure water. Three different tests with three replicates each, performed on ultra-pure water using the same methodology are presented in the figure. The analysis of the isotherms reveals significant differences

involving irreproducibility of the shape of the isotherms for the different tests including the collapse phase, which prevented a proper interpretations of the results.

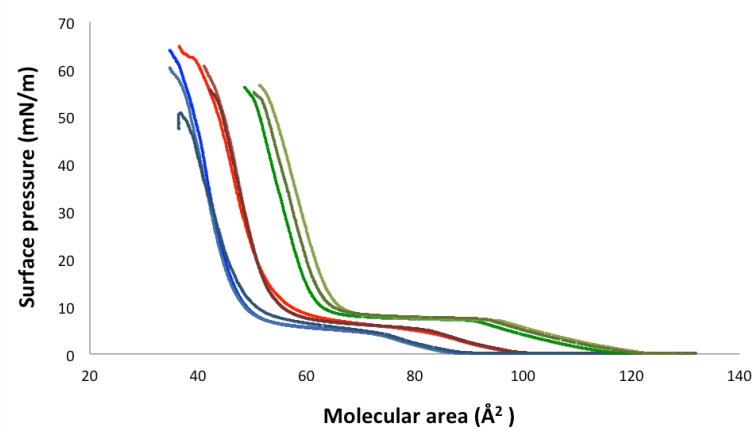

Figure 11: Pressure-area isotherms of DPPC monolayers in ultra-pure water (lines with the same color represent replicates of the same experiment using the same conditions and experimental procedure).

Since the Langmuir-Blodgett technique is extremely sensitive, the accumulation of insoluble impurities at the surface of the water has always a significant effect. These molecules remain and accumulate at the interface, changing the molecular concentration or even affecting the intermolecular interactions between the film molecules, which induces changes on the isotherms profile. Thus we concluded that the differences observed between replicates were related to subphase contamination by surface-active impurities. We concluded that the source of these contaminations aroused from air-borne particles accumulation and from the reuse of the same subphase in different assays. We observed that despite of cleaning the surface of the subphase after each test, the risks of contamination of lipids from older assays were high. When the subphase was not replaced by fresh water and when the barriers and the trough were not properly cleaned before each study, the isotherms were more susceptible to variations. The same behavior was observed when the films were exposed at the air-water interface during long periods of time as the probability of deposition and accumulation of air-borne particles was higher. In order to eliminate these sources of contamination, we decided to clean the barriers and the tank with chloroform and to use fresh water before performing each test. In addition, we have made sure that the environment around the equipment was always free of dust and that the time of evaporation after the spreading process was always the same.

As discussed in the introduction, the collapse phase results from the compression of insoluble films beyond the minimal area available to accommodate the molecules in the

2D plane. Moreover, in normal collapse processes, the surface pressure might remain constant and a horizontal plateau might be formed **(Notter R. H., 2000)** (Figure 12).

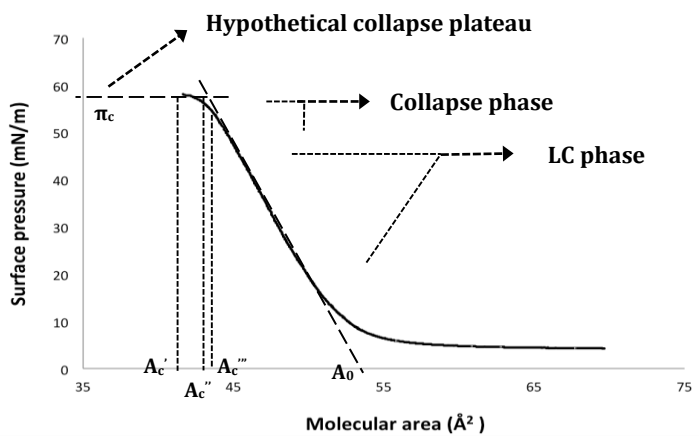

Figure 12: Collapse pressure (π_c) and collapse area (A_c) of a DPPC monolayer. Being the A_c''', the area where the isotherm departs from its steepest slope; A_c'', the area where the collapse plateau intersects the line of steepest slope; and A_c', the area where the maximum pressure (π_c) is reached. Adapted from**Notter R. H., 2000**.

On Figure 11 no horizontal plateau was observed but, instead, a slightly increase of the surface pressure. Therefore, we suggest that the presence of experimental errors like interface contamination and leakage effects might also be leading to the irreproducibility of the collapse pressures and areas. From the analysis of the results reported in literature it is evident that the collapse mechanism of the DPPC monolayers is still not well understood. Studies have been describing different interpretations of this phase. Duncan and Larson concluded that variations regarding experimental isotherms have been leading to misinterpretation of the real point of collapse phase of DPPC monolayers **(Duncan S. L. and Larson R. G., 2008)**. Wustneck et al. concluded that under circumstances as film over-compression, the monolayers can suffer gradual rearrangements that allow changes in the surface pressure that lead to premature collapse phases **(Wustneck N. et al., 2000)**. As the study of the collapse phase is not essential to accomplish the objectives of our work, we performed our tests by taking into consideration the reproducibility of our results. Hence, we have decided to perform our experiments at lower compression rates of $10 cm^2.min^{-1}$ in order to avoid premature collapse. Considering the structural features of DPPC and the apparatus limitations earlier discussed, the highest surface pressure that can be reached during the compression of a DPPC monolayer in the conditions at which we are working are, as shown in Figure 13, approximately 60 $mN.m^{-1}$.

The concentration of the molecules added to the subphase is essential for a correct evaluation of the pressure-area isotherm during the compression. This parameter is defined in the software used to store and correlate the data from the experimental studies. If the concentration of the DPPC solution is not correct, the number of molecules added to the subphase will not be the same as the number of molecules used by the software during the evaluation of the interfacial changes, and irreproducibility problems will arise. As for each of the three tests different solutions of DPPC were used, we concluded that the large variability observed in the isotherm between different tests was due to errors on the concentration of the DPPC solution. Efforts were made in order to eliminate variations on the concentration of the DPPC solutions. Therefore, we decided to prepare fresh solutions of DPPC every week. After the solution preparation, several isotherms were performed in order to evaluate the possibility of contamination or to identify old and new errors on the experimental preparation. The solution was used during the same week, and precautions were taken in order to minimize the alteration of the solution concentration or purity. Between each assay, the solution was tightly sealed in order to avoid chloroform evaporation, which could change the concentration along time. At the end of the experiments, the solution was kept at constant temperature (5ºC) in the fridge. At the beginning of each day, one isotherm was performed to compare and validate the quality of the solution. If the quality of the solution changed, a new solution was prepared and validated before further studies. Figure 13 shows the reproducibility achieved after taking in consideration all the considerations discussed above.

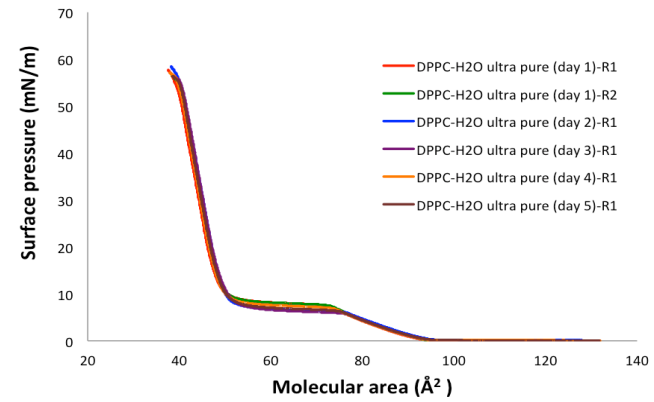

Figure 13: Langmuir π-A isotherms of a DPPC monolayer spread on the air-water interface. The solution was prepared and tested at the beginning of each day, during 5 days, aiming its validation, thus minimizing potential problems and guaranteeing the reproducibility of the results.

Furthermore, notice should be made that recent studies carried out by our collaborators at IFSC-USP in a 10000 clean room at room temperature, 22 (±1 °C)have confirmed our results.

3.3 – Dynamic packaging of DPPC monolayers

Taking into consideration the natural composition of cell membranes and the natural abundance of phosphatidylcholine derivate, especially in the outer leaflet of the cell membrane, we decide to use Langmuir films of DPPC phospholipids as a cellular membrane model. The chemical structure of DPPC is constituted by an uncharged head group formed by two spatially separated oppositely-charged moieties, a positive choline moiety linked to a negative phosphate group (polar head), and two saturated alkyl chains with 16 carbons (non-polar tail)– see inset of Figure 14. The use of the DPPC allows a close representation of the external leaflet of the cell membrane, and thus a reasonable simulation of the interactions acting between the ionic liquids and the living cell membranes.

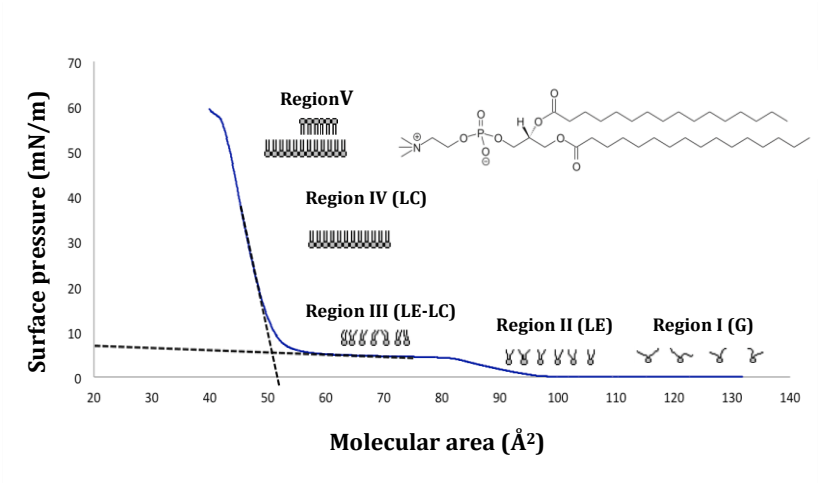

Figure 14. Langmuir π-A isotherms of a DPPC monolayer spread on the air-water interface. Inset - molecular structure of DPPC.

Surface pressure-area isotherm measurements are the conventional way to characterize the phase behavior of Langmuir films. Figure 14 shows the surface pressure-molecular area isotherm of DPPC monolayer on a pure water subphase as well as the schematic representation of the corresponding stages of packing of the molecules during the compression of the film. Similarly to the study of stearic acid mentioned in the introduction, as the DPPC solution is spread on the air-water interface, the molecules assume a freely packed form at the water surface. At this stage, the molecules behave as a

2D gas, being organized in a way that there are no interactions between them. This phase is classified as gas phase and is represented by a perfectly horizontal plateau at a surface pressure equal to 0mN.m^{-1}(**Region I**). As the DPPC monolayer is being compressed, the molecules start to approach in a way that they start to feel the closest molecules (approximately between 80 to 100Å^2). In this packaging phase, the molecules assume the behavior of a 2D liquid classified as liquid-expanded phase (LE), which is graphically represented as the first plateau to the far right of the isotherm (**Region II**). By further compression of the monolayer, the molecules get closer to each other and physical contacts are established (between 80 to 50Å^2 approximately). This stage is classified as the liquid-expanded/liquid-condensed phase transition (LE-LC), and it is graphically represented in the isotherm as the second plateau, observed around 6mN.m^{-1} (**Region III**). As the monolayer is being compressed to higher values of pressure, the DPPC molecules reach a high stage of organization in which the area around each molecule reaches a minimum and the molecules form an ordered and compacted film (between 50 to 45 Å^2, approximately). In this packaging stage, the molecules assume the behavior of a 2D semicrystaline phase. This phase is classified as a liquid-condensed phase and, similarly to the solid phase of the stearic acid, it is graphically represented by a linear relationship between the surface pressure and the molecular area (**Region IV**). Further compression of the monolayer causes the rupture of the DPPC monomolecular film, allowing the formation of aggregates, lipids dissolution and/or the formation of bilayers and/or multilayers (about 45Å^{2}approximately). This stage is classified as the collapse phase, and it is graphically represented as a final kink of the isotherm, found at surface pressures around 60mN.m^{-1} (**Region V**). For pure DPPC monolayer on ultrapure water, a limiting molecular area was obtained at around 51,1 Å^2.molecule^{-1}.This value is in agreement with the estimated minimum area of DPPC headgroups on a monolayer in a liquid condensate phase (approximately 50Å^2)**(Gennis R. B., 1989)**, and is consistent with data reported in literature **(Pavinatto F. J. et al., 2007).**

3.4- Interaction between [C$_6$mim]Cl with DPPC monolayer

It is known that the pressure-area isotherms are a function of the surface pressure, surface area and temperature. As discussed in the introduction, this correlation is the result of a thermodynamic relationship that acts upon the molecules during the compression and packing of the monolayer. When measured accurately and under equilibrium conditions this relationship ought to be universal and specific of the

superficial film molecules **(Duncan S. L. and Larson R. G., 2008).** Based on that, and in case that there are interactions acting between the DPPC monolayers and the ionic liquids, the thermodynamic relationship acting during the compression of pure DPPC monolayers is affected, causing changes on the packaging kinetic that lead to changes in the pressure-area isotherms. In our studies, the interactions of the DPPC monolayer with different [C_6mim]Cl concentrations added to the aqueous subphase were initially studied using the surface pressure-molecular area isotherm technique. The [C_6mim]Cl has been selected to analyse the interactions of the alkyl chain length with the DPPC monolayers as it represents the alkyl chain length at which the EC_{50} values of the imidazolium ILs family present a remarkable increase. Figure 15 shows the influence of the [C_6mim]Cl in the subphase on DPPC monolayers at the air-water interface

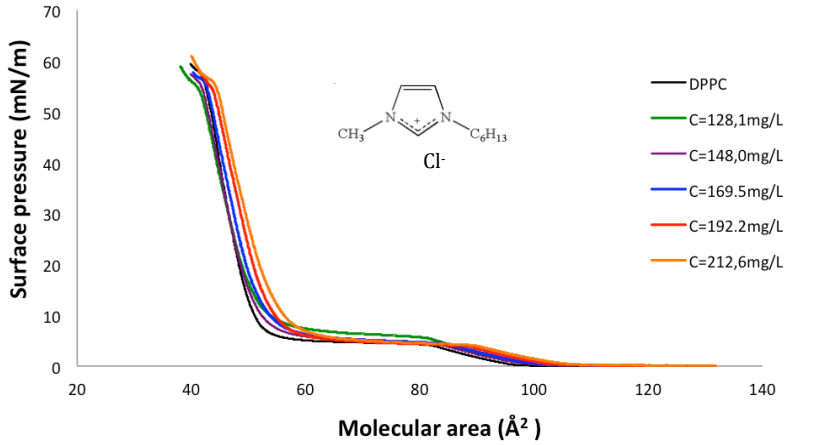

Figure 15: Pressure-area isotherm for DPPC monolayers formed in ultra-pure water and, formed in a subphase containing the ionic liquid [C_6mim]Cl at the concentration between 128.1 mg.$L^{-1}$and 212,6 mg.L^{-1}.

Considering our interest in using the LB technique to get complementary information at molecular level regarding the toxicity of ILs, we took as reference concentration that of EC50 of [C_6mim]Cl (170 mg/L). Comparing the DPPC pressure-area isotherms obtained on ultrapure water with those obtained in the presence of [C_6mim]Cl, significant changes on the isotherms shape were observed. The effect of the [C_6mim]Cl was found to be significant as the results obtained indicate that it perturbs the LE transition and the LC phase.By a general analysis of the isotherms we were able to observe that as the [C_6mim][Cl] concentration increases (from 128,1 to 212,6 mg L^{-1}), the transition region of G phase to the LE phase is shifted to bigger molecular areas. Furthermore, the LE-LC transition phase converges to similar values of those obtained on

pure DPPC monolayers and the LC phase is shifted to higher values of area *per* molecule. As an illustration of the effect of the [C_6mim]Cl on the DPPC monolayers, in Figure 16 and 17 are depicted the variations of the area *per* molecule and the surface pressure as a function of the ILs concentration for a fixed surface pressure and a fixed area *per* molecule respectively.

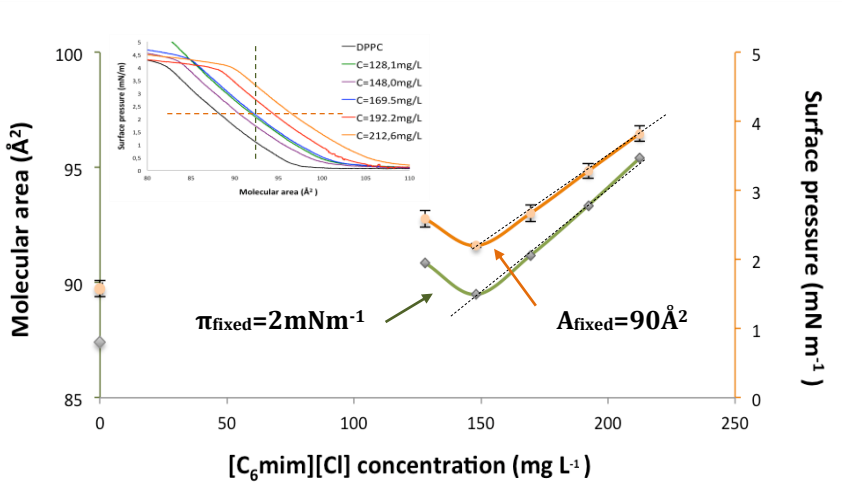

Figure 16: Surface pressure variation at the fixed area of 90Å²mol^{-1} and molecular area at the fixed pressure of 2mN.m^{-1} as a function of the [C_6mim][Cl] concentration.

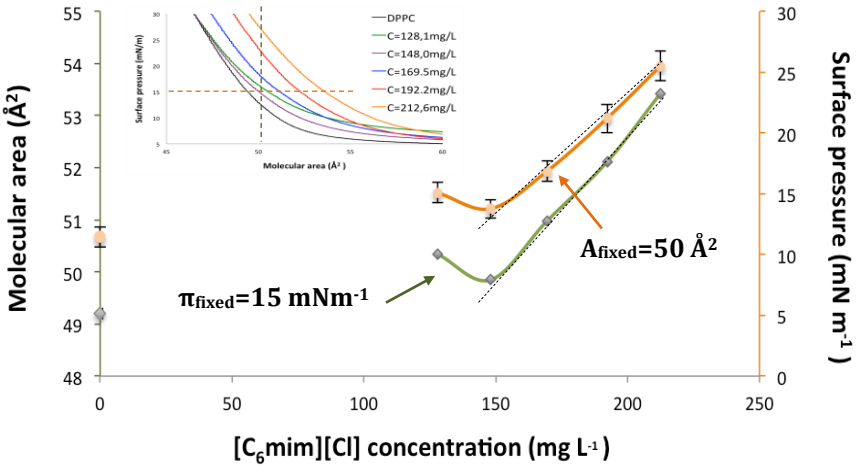

Figure 17: Surface pressure variation at the fixed area of 50Å²mol^{-1} and molecular area at the fixed pressure of 15mNm^{-1} as a function of the [C_6mim][Cl] concentration.

On these figures it is possible to observe that above the concentration of 148,0 mg.L^{-1} the changes in both LE phase (Figure 16) and LC phase (Figure 17) caused by the [C_6mim]Cl follow a linear increase. The fact that this increase is proportional to the concentration of

[C_6mim]Cl suggests the inclusion of the [C_6mim]Cl molecules inthe monolayer. Although not observed in the range of concentrations tested, this approach can be useful, not only to assess the changes suffered by the monolayers, but also to evaluate the saturation concentration of the [C_6mim]Cl in the lipidic films. This phenomenon involves the reversibility of the expansion effect observed and reported before, which might occur above certain concentrations of [C_6mim]Cl in cases where: i) the monolayer assumes residual charge as a result of the adsorption of the charged molecules, that might repel and avoid the adsorption of new molecules; ii) the ions interact, to some extent, with all ions of opposite charge in their vicinity, reducing the strength of their intramolecular interactions and, therefore, the range over which their effects are significant on the expansion of the DPPC monolayers **(Pavinatto F. J. et al., 2007).** The saturation concentration might be of crucial importance not only for the possible correlation with the effects reported so far, but also with many others that at this point we are unable to test or understand (e.g. kinetics of adsorption and mechanisms of toxicity). Therefore, in future studies, this issue must be addressed by testing a higher range of concentrations.

From the analysis of Figures 15 to 17 we concluded that LE phase seems to be favoured by the presence of [C_6mim]Cl as the G-LE transition occurs at larger values of areas. Thus, we suggest that the [C_6mim]Cl might be affecting the kinetics of the nucleation process of the DPPC monolayer and that the formation of LE phase domains is promoted. This might be due to inductive forces such as electrostatic interactions between the $[C_6mim]^+$ and the positive ammonium group of the DPPC polar head, that might increase the density of forming DPPC domains at the G phase allowing early LE transitions. Indeed, it is known that the growth of the DPPC domains begins at lower pressures and continues evolving with the increase of the pressure until they achieve their fundamental shape and size at the LC phase **(Cary W. and T. Kyle Vanderlick, 1997)**. In this context, it is obvious that the morphology and size of the LC phase domains might be typically defined by the phenomenon ruling the coexistence region. Many studies about the effects of specific molecules on DPPC Langmuir monolayers at the air-water interface have shown that their interactions, making or not changes in the LC phase, are correlated with significant changes on the LE phase **(Aroti A. et al., 2004)**. Thus, we conclude that although [C_6mim]Cl might be able to induce the formation of LE phase domains, it does not affect significantly the morphology (size and shape) of the DPPC domains. This conclusion is based on the convergence of the plateau of the LE-LC phase transition during the increase of the [C_6mim]Cl concentration towards similar values to those registered for the DPPC monolayers in ultrapure water. As far as we know, this behaviour is quite unusual in

literature considering that, with the increase of the [C_6mim]Cl concentration, this convergence is later followed by displacements of the LC phase to higher molecular areas. In this sense, these results suggest that the conditions at which the [C_6mim]Cl is able to interact with the lipidic domains only occurs at higher levels of organization. As at high surface pressures the isotherms are not converging to molecular area values as those of pure DPPC monolayers, we propose that the monolayer expansion shown may be caused by the establishment of strong local interactions between the DPPC molecules and the IL that allow the [C_6mim]Cl to remain in the monolayer. Since many studies have shown that the presence of NaCl in the subphase causes little to no shift in the DPPC pressure-area isotherms **(Aroti A. et al., 2004; ShapovalovV. L., 1998)**, we propose that the interactions between the DPPC monolayers and the [C_6mim]Cl might be predominantly ruled by the cation $[C_6mim]^+$. However, the contribution of Cl^- to structural changes of the DPPC monolayer should also be considered as several studies have found slight changes of the isotherm shape and area per molecule for large variations of the ionic strength **(Zaitsev S. Y. et al., 1996)**.

3.5-In-plane elasticityof DPPC and DPPC-[C_6mim][Cl] monolayers

Besides the morphological characterisation made by the direct analysis of the pressure-area isotherms, it is also possible to obtain an insight about the mechanical properties of the DPPC monolayers by calculating their in-plan elasticity or compressibility modulus. This additional approach provides valuable information about the elasticity and compressibility of the monolayers, which defines the ability of these structures to change and restore their physical morphology during the action of external forces **(Khattari Z. et, al. 2011).** In presence of specific molecules in the subphase, the changes of monolayers elasticity and compressibility are of much importance in the interpretation of the interactions acting between perturbing agents and the lipidic films. In this work, these evaluations were made by the calculation of the compression modulus of the DPPC films at the air-water interface. The compressibility modulus of an amphiphilic monolayer at the air-water interface is mathematically defined by Equation 2 and was calculated using the pressure-area isotherms data. Notice that a high value of Cs^{-1} indicates that the monolayer has a higher elasticity (flexible morphology) and vice versa. In addition, it is predictable that the highest compressibility modulus will be found at high surface pressure during the LC phase as the monolayers are more compact. Hence, it involves large reduction of the surface tension for a small decrease of molecular area. The Cs^{-1}

values of a DPPC monolayer on ultra-pure water were calculated and then analysed as a function of the molecular area. To make the interpretation of these results easier the corresponding pressure-area isotherms were also plotted (Figure 18).

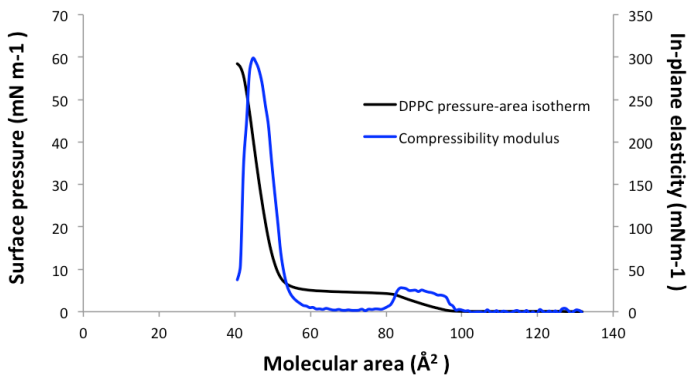

Figure 18:Π andC_s^{-1} as a function of areaof DPPC monolayers on ultra-pure water.

From the evaluation of the Cs^{-1}-*A* curve it is possible to identify analogies between the different regions of compressibility to the phase transitions of the pressure-area isotherms. In general, it is possible to observe that at the beginning of the compression the value of elasticity of the monolayer is zero, which is in agreement with the packing level of the film at the G phase. Moreover, at the value of 100Å² the film elasticity started to increase reaching a maximum compressibility of 27,93mN.m^{-1} at 84Å². This compressibility phase is characteristic of the LE phase and it correlates with the increase of the compaction and rigidity of the film, resulting from the formation of LE domains. As the monolayer is further compressed, the elasticity decreases until 3mN.m^{-1}, remaining then constant until the area of 58Å² (LE-LC phase transition). At the area of 59Å² the elasticity of the monolayer starts to increase linearly achieving a final maximum of 300mNm^{-1} at 45Å² (LC phase). As the monolayer is compressed beyond the maximum compressibility, the elasticity drops, making the monolayer more susceptible to morphological deformations **(Wang Z. and Yang S., 2009).** Another way to evaluate the compressibility modulus of monolayers is to plot it as a function of the surface pressure (Cs^{-1}- π). Although this study does not provide direct evidence for the existence of phase transitions, it gives an important support for the interpretation and infer of different states of molecular arrangements, interaction and aggregationresulted from the insertion of molecules of a second component in superficial monolayers **(Schmidt T. F. et al., 2008)**(Figure 19).

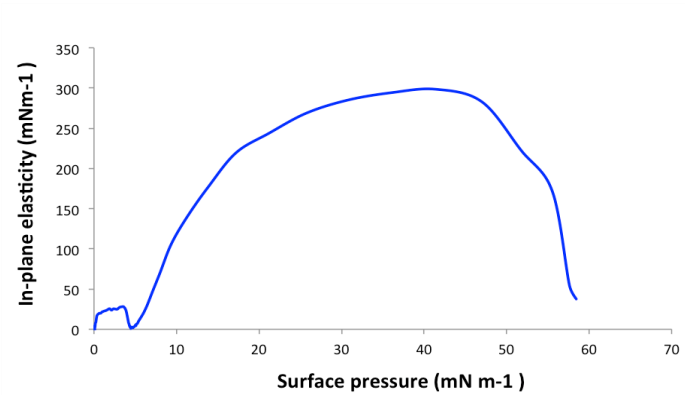

Figure 19: Compressibility modulus as a function of the surface pressure (Cs^{-1}- π) of the DPPC monolayer at the air-water interface.

We highlight the example about the surface pressure at which the maximum compressibility is reached (between 35 to45 mNm^{-1}). This pressure is extremely important, as it represents the pressure frontier between flexible and rigid monolayers and embodies an important proximity to the values described for the biological membranes **(Marsh D., 1996)**. Thus it gives us a way to compare and interpret the experimental data obtained from our studies with those from toxic tests for living cells. To better understand the effects of [C_6mim]Cl on the monolayer stability and clarify their interactions with the DPPC Langmuir films, the compressibility modulus data were examined. The Cs^{-1} values of the monolayers formed in presence of an increasing concentration of [C_6mim]Cl in the subphase were calculated and are plotted as a function of the molecular area and the surface pressure in Figure 20.

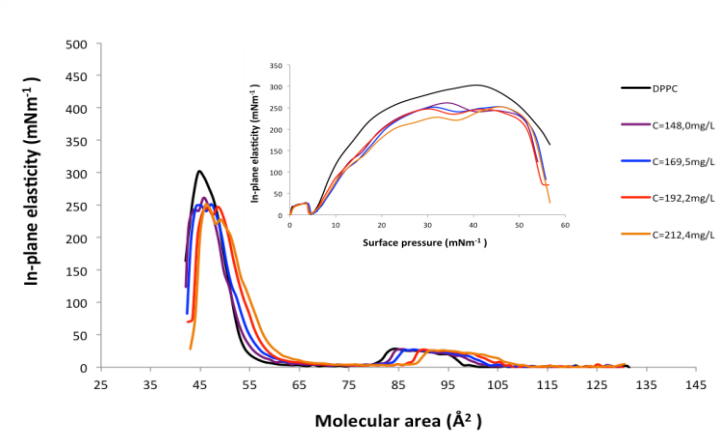

Figure 20: In-plane elasticity (Cs^{-1}) of DPPC monolayers formed in the presence of different concentrations of [C_6mim]Cl as a function of the molecular area and the surface pressure (Cs^{-1}-*A* and Cs^{-1}- π).

Figure 20shows that the DDPC monolayers elasticity is affected by the presence of the [C_6mim]Cl on the subphase. It can be seen that the [C_6mim]Cl induces slight shifts on the typical compressibility of the packing degree of the DPPC monolayer. We observed that the increase of the compressibility at the LE phase is moved to higher areas, which is justified by the earlier transition of G phase to the LE phase. Moreover, the values of C_s^{-1} of the LE-LC phase transition converge to approximately the same value as the pure DPPC (around 26 mN.m^{-1}± 2), which reflect the similar packing profile observed on the pressure-area isotherms. In addition, the adsorption of [C_6mim]Cl onto the DPPC monolayers causes the decrease of the maximum C_s^{-1} from a value of approximately 300 mN.m^{-1} for pure DPPC films to values between 261 and 250 mN.m^{-1}. The results obtained show that in presence of the [C_6mim]Cl the monolayer assumes a lower elastic morphology, suggesting a more rigid monolayer with a more condensed and organized physical state that might turn the monolayer more susceptible to morphological deformations. We conclude that the [C_6mim]Cl was able to interact with the DPPC monolayer affecting the packing of the lipids.

3.6 – Compression-Expansion Hysteresis of DPPC monolayers

During compression processes, surfactant monolayers at the interface air-water can suffer phenomena of partial ejection and squeeze out of material even if under surface pressure below the collapse. Moreover, during the expansion processes, these phenomena can be partially/fully reversible (dynamic re-spreading) **(Notter, R.H., 2000)**. As the ejection and the integration of the material can present different rates between compression and expansion, several differences can be observed on the isotherms of both processes. If after the compression, the area occupied by the molecules is increased, the expansion isotherm is displaced to lower values of area and a hysteresis profile is obtained. The study of hysteresis phenomena using cycles of compression and expansion is called isocycles and allows us to evaluate both reversibility and stability of the films under specific conditions. The study of DPPC monolayer hysteresis in presence of ILs is especially important, since it could give us direct indications of hysteresis caused by the interaction of the ILs with the monolayers. If [C_6mim]Cl is able to interact with the DPPC monolayer, the dynamics of re-spreading of the material is affected thus, the levels of hysteresis of the lipidic films are altered. The stability and reversibility of DPPC monolayers, with and without the presence of [C_6mim]Cl in the subphase were studied

using the isocycles approach. The studies performed with a DPPC monolayer on ultra-pure water and in the absence of [C_6mim]Cl are shown on Figure 21.

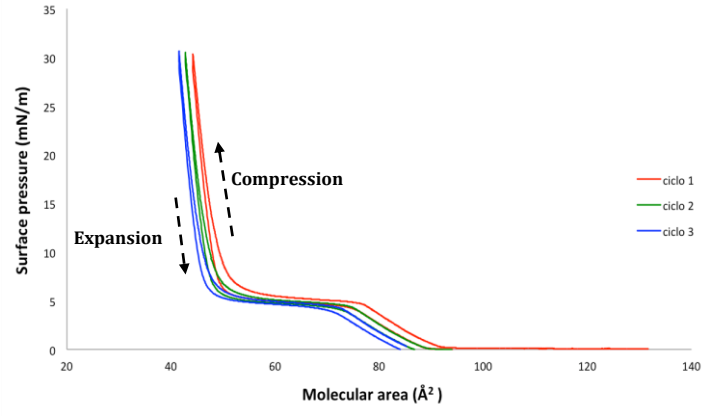

Figure 21: Hysteresis curves of pure DPPC monolayers formed in ultra-pure water.

Figure 21 demonstrates that the DPPC monolayers in ultra-pure water were stable, being characterized by a reversible packaging process. However, it is observed that the shape of the isotherms was not totally similar between the cycles of compression and expansion. In addition, it should be noted that in the successive cycles, the isotherms were slightly displaced to smaller values of area. Although not very significant, the hysteresis behavior observed suggests, as explained before, that there-spreading of DPPC molecules at the interface was not fully efficient. These results suggest the formation of three-dimensional aggregates and/or the squeezing out of DPPC molecules during the compression.

The isocycles of DPPC monolayers in presence of [C_6mim]Cl for 140, 170 and 212mg.L^{-1} are shown in Figures 22, 23 and 24, respectively.

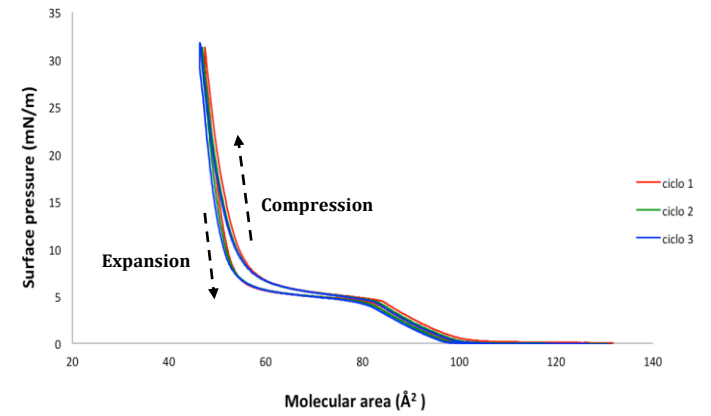

Figure 22: Isocycles of pure DPPC monolayers in the presence of 140,0mg.L^{-1} of [C6mim]Cl.

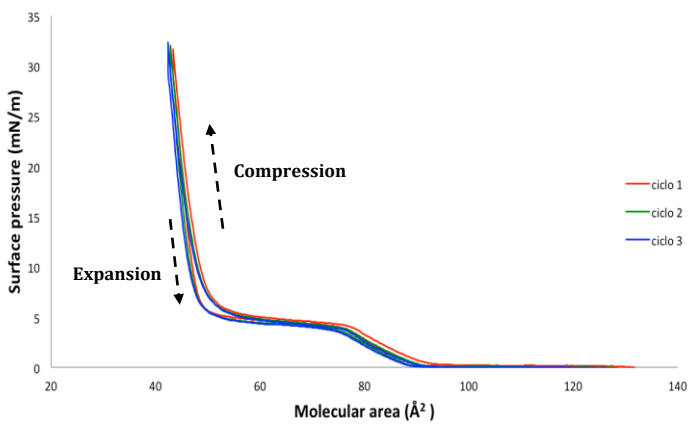

Figure 23: Isocycles of pure DPPC monolayers in the presence of 169,5mg.L^{-1} of [C_6mim]Cl.

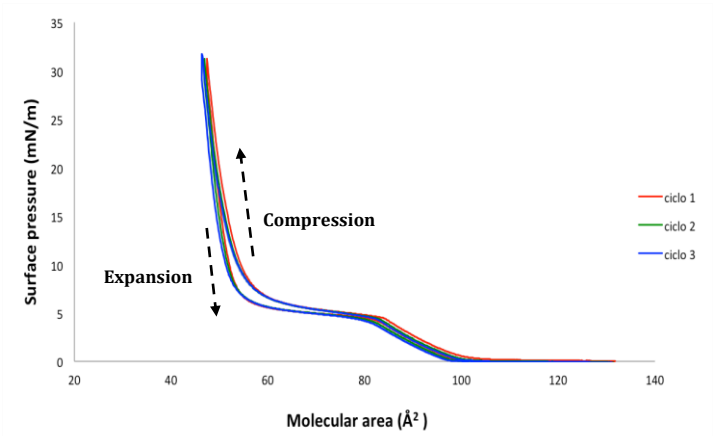

Figure 24: Isocycles of pure DPPC monolayers in the presence of 212,4mg.L^{-1} of[C_6mim]Cl.

By the analysis of the isocycles in Figures 22 to 24,we observed that in the presence of [C_6mim]Cl, the hysteresis of the DPPC monolayers is slightly reduced when compared with the films obtained for DPPC in ultra-pure water. Moreover, after the first compression cycle, the expansion/compression profiles remained unchanged and no displacement of the isotherm to lower values of area occurred. This means that during the expansion of the monolayer, the lipids aggregated or squeezed-out are more efficiently re-spread in the presence of this specific IL than in ultra-pure water. In this sense, it is possible to conclude that [C_6mim]Cl affects not only the phase behavior and elasticity of the DPPC monolayers, but also the dynamics of the re-spreading process, inducing higher levels of stability and reversibility of the lipidic films.

3.7 - Study of the interaction between [Chol]Cl and DPPC monolayers

As discussed in the introduction it has been recently proposed that the cholinium family exhibits a different mechanism of toxic action comparatively to the imidazolium counterparts. In order to investigate these mechanisms, several studies regarding the interactions of DPPC monolayer with different concentrations of [Chol]Cl, were performed (Figures 25 and 26). It was observed that, when [Chol]Cl is added in the subphase, both the pressure-area isotherm and the compressibility modulus of the DPPC monolayer suffered alterations.

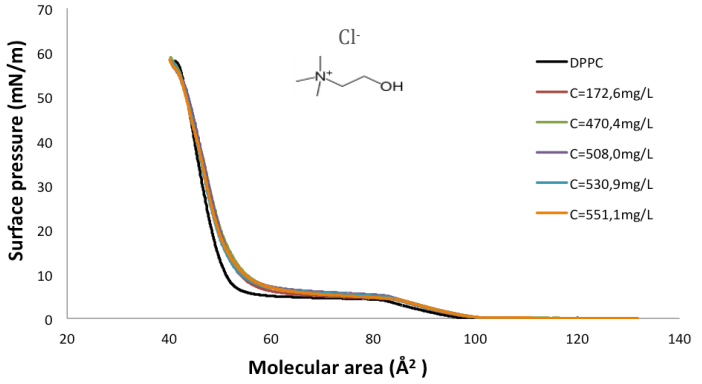

Figure 25. Representation of the pressure-area isotherms for pure DPPC monolayers on an aqueous subphase and in the presence of [Chol]Cl, from 172.6 to 551.1 mg .L^{-1}.

Figure 25 shows that, despite the small changes observed, the pressure–area isotherm of the DPPC monolayers is not affected when the concentration of [Chol]Cl is increased. Thus, it was concluded that, as opposed to the [C_6mim]Cl results, the effect of this cholinium structure on the DPPC monolayers was not dependent of the concentration tested. The slight shift of the isotherm at the beginning of the LC phase, suggests that [Chol]Cl is capable of interacting and probably of being incorporated into the head group region of the DPPC monolayer. However, the convergence of the solid phase suggests that the penetration and expansion of the monolayer at high pressures is reversible, and that the [Chol]Cl is expelled from the film. The effect of cholinium in the film elasticity was also investigated through the calculation of the compressibility modulus of the DPPC monolayer, which was then plotted as a function of the molecular area and the surface pressure (Figure 26).

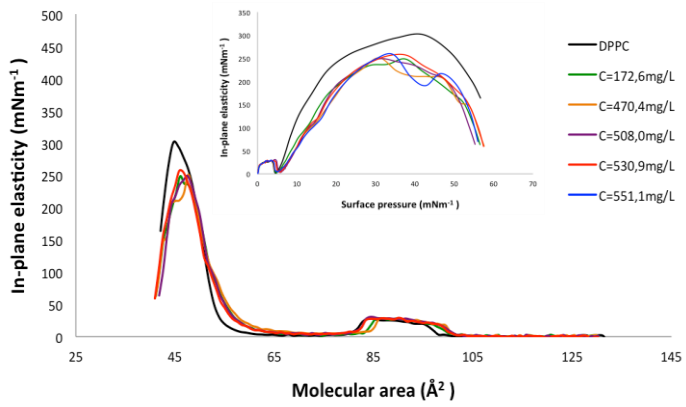

Figure 26: In-plane elasticity (CS^{-1}) of DPPC monolayers formed in the presence of different concentrations of [Chol]Cl, as a function of molecular area and surface pressure.

Figure 26 shows that [Chol]Cl induced significant differences on the film compressibility modulus at specific stages of the DPPC packing. The displacement at the beginning of the LC phase for higher area values in the films containing [Chol]Cl is a reflection of the expansion imposed by the ionic liquids on the DPPC films. However, contrary to what was observed for [C_6mim]Cl, the change on the compressibility observed in the LC phase converge to values of pure DPPC monolayers. This parameter is in agreement with the conclusions taken from the analysis of the isotherm shown in Figure 25 regarding the ejection of [Chol]Cl from the monolayer at higher pressures. Similarly to the [C_6mim]Cl, the incorporation of [Chol]Cl in the films seems to cause a reduction of the maximum value of the film elasticity, which was about 300mN.m^{-1} for the pure DPPC film in ultra-pure water and between 248 and 251mN.m^{-1} for films containing [Chol]Cl. These values suggest that the incorporation of [Chol]Cl might interfere with the dense packing of the polar head group and change the fluidity of the lipidic monolayers. It can be seen on the Cs^{-1}- π plot that at pressures between 0 and 30 mN.m^{-1} as well as between 50 and 60mN.m^{-1} the compressibility modulus remain similar between the different concentrations tested. However at pressures between 30 and 50mN.m^{-1} significant changes are observed. This effects of the [Chol]Cl on the DPPC monolayers at this specific pressure is special interesting as this pressure is more similar to the biological membranes. We propose that after adsorption on biological membranes, the [Chol]Cl might not be able to remain bonded to the monolayer, however, this proposal does not invalidates the ability of cholinium to penetrate the membrane cell, for example by diffusion processes.

3.8 - Study of the alkyl chain effect on DPPC monolayers

As discussed in the introduction, the alkyl chain length is being correlated with some of the toxic effects obtained from the interaction of ionic liquids with cell membranes. This toxic effect is often described as a disturbing interaction between the alkyl chain and cellular membrane molecules (e.g. membrane phospholipids), leading to membrane instability and function losses. It is well known that the toxicity of the ionic liquids is higher with the increase of the alkyl chain, phenomenon classified as the "side chain effect", being the number of carbons at which the alkyl chain has no increased influence on the toxicity described as "cut-off effect". In order to better understand these effects, several studies were performed, by testing the effects of different ILs with alkyl chain lengths distinct of the already discussed C6 (C2, C4, C8 andC10) in terms of the DPPC pressure-area isotherms (Figure 27).

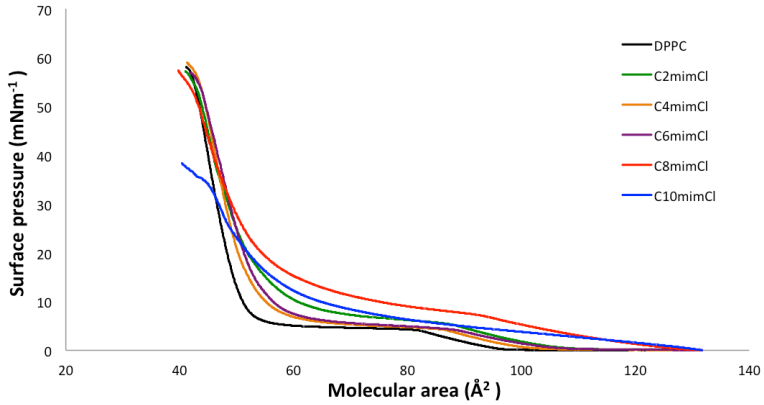

Figure 27. Pressure-area isotherms for pure DPPC monolayers on an aqueous subphase and in the presence of [C_2mim]Cl,[C_4mim]Cl, [C_6mim]Cl, [C_8mim]Cl and [C_{10}mim]Cl at 122.77, 172.4, 195.4 and 220.6 mg/L respectively.

Comparing the DPPC pressure-area isotherms on ultra-pure water with those obtained with imidazolium-based IL with different alkyl chain lengths, significant changes were found. We observed that the increase of the alkyl chain length induced changes in the pressure-area isotherm, as well as in the minimal area occupied by a DPPC molecule at the LC phase. It is possible to observe from the analysis of Figure 27 that most of the ILs tested behaved as theoretically expected.The increase of the area filled by one molecule of the lipidic film in the condensed phase at zero pressure was 57, 54, 56, 58 and 62$Å^2$.molecule^{-1}, for [C_2mim]Cl,[C_4mim]Cl, [C_6mim]Cl, [C_8mim]Cl and [C_{10}mim]Cl, respectively. Thus, we concluded that with the addition of these ILs to the subphase, the films are more expanded, and that this expansion gradually increases with the alkyl chain length. As concluded by

the analysis of the isotherm and the value of the minimal area at the LC phase, [C_2mim]Cl showed higher film expansion than the [C_4mim]Cl and [C_6mim]Cl. These results are not coincident with the behavior expected for [C_2mim]Cl, which means that possible distinct mechanisms are acting. Regarding the differences observed between [C_4mim]Cl and [C_{10}mim]Cl, we concluded that the effect of the increase of the alkyl chain length is regulated by their lipophilic characteristics. In this context, the number of carbons may play an important role on the impact and nature of the interactions. The transition of the surface-active features expected between ionic liquids of small and long alkyl chains are clear on the isotherm studies. This transition is revealed on the isotherm profile of [C_8mim]Cl, which is structurally often cited as the transition of the surfactant properties of the ILs. We propose that due to the lower degree of solubility of their alkyl chain in water, the [C_8mim]$^+$will naturally migrate from the subphase to the interface adsorbing and interacting with the DPPC monolayers. Notice that as opposed to the ionic liquids with small alkyl chain the [C_8mim]$^+$ is able to induce changes in all packing phases, which suggests their ability to surpass earlier the electrostatic repulsions acting between the positive ammonium group that might be avoiding the penetrations of ionic liquids with C≤6. Yet, comparatively to the [C_{10}mim]Cl it is possible to observe that the changes induced by [C_8mim]$^+$ do not totally alter the phase behaviour of the DPPC monolayer. In turn, [C_{10}mim][Cl] proved to be extremely efficient in the modification of the DPPC molecules arrangement. We suggest that its alkyl chain will strongly interact with the films through hydrophobic and dipole interactions inducing not only the expansion of the membranes as reported before, but also earlier collapse phases. Its higher ability to accumulate on the films might be followed by higher changes in the stability and elasticity of the films. Figure 28 shows the [C_{10}mim]Cl induced monolayer hysteresis.

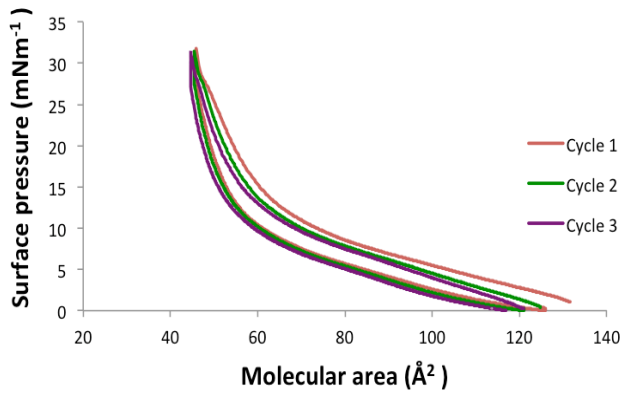

Figure 28: Hysteresis curves of DPPC monolayers in the presence of [C_{10}mim][Cl] in the molar concentration referent to [C6mim][Cl] EC50.

The profile variation on the hysteresis isotherm registered for the DPPC monolayers in the presence of [C_{10}mim]Cl may be associated with selective squeeze-out of phospholipds from the mixed film formed at the surface after the adsorption of the [C_{10}mim]$^+$. These effects might arise from the unbalance among cohesion phenomena related to the structural configuration of the DPPC monolayers at closely packed liquid condensed states formed under compression (Figure29).

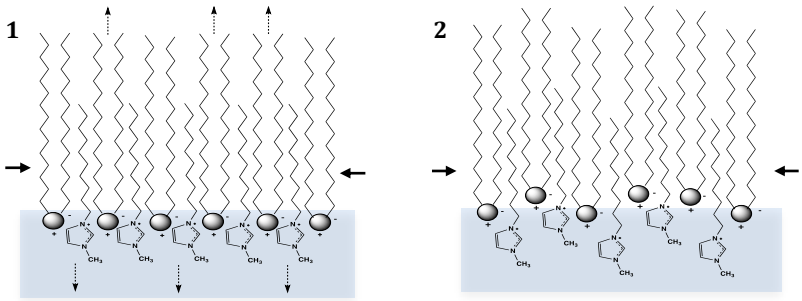

Figure 29: Representation of a possible mechanism of squeeze-outof DPPC molecules during the monolayer compression in the presence of the [C_{10}mim][Cl]. When the mix DPPC+[C_{10}mim][Cl] is compressed, some constituents can be selectively injected or squeezed out of the interface.

As the DPPC phospholipids and the alkyl chains of [C_{10}mim]$^+$ do not have the same free energy and equal mobility at the surface, the molecules with lower affinity for the interface will tend to be preferentially ejected from the film during the compression. The curves show that after the first compression a reversible behaviour is achieved which indicates that the [C_{10}mim]$^+$ remains in the Langmuir film. As no significant reduction of the area occupied per molecules was observed between the successive compressions and expansion cycles, no signals of material loss were observed, thus we concluded that [C_{10}mim][Cl] is not able to induce the phospholipids dissolution in the subphase and that during the expansion process the DPPC returns to the interface (Figure 30).

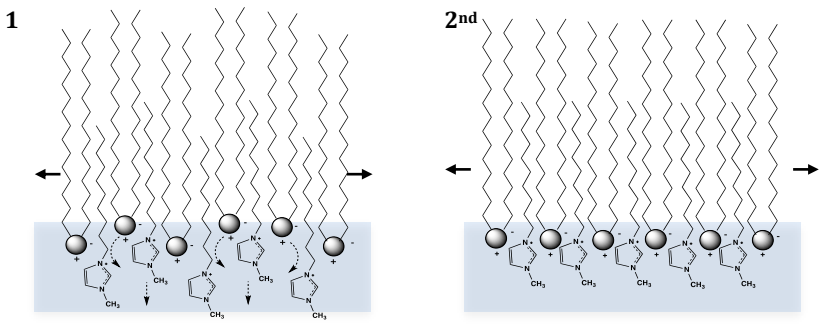

Figure 30: Representation of the integration of the squeezed-out DPPC molecules during the monolayer expansion.

From a general analysis of the compressibility modulus of the DPPC monolayer present in the Figure 31, we were able to observe that the elasticity of the lipidic films decreases with the increase of the alkyl chain.

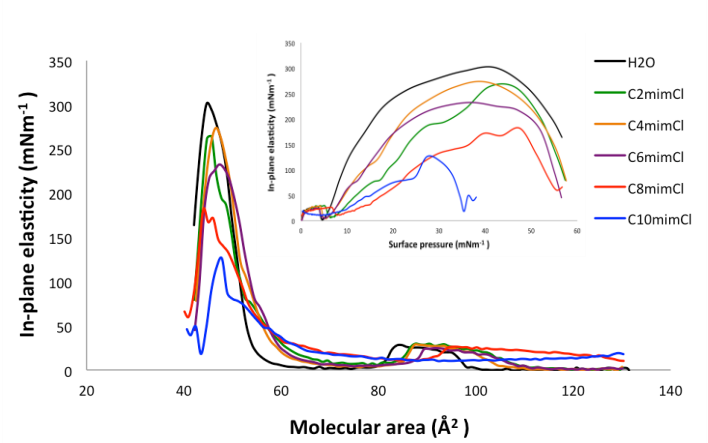

Figure 31. In-plane elasticity (C_S^{-1}) of DPPC monolayers formed in the presence of [C_2mim][Cl], [C_4mim]Cl, [C_6mim]Cl, [C_8mim]Cl to [C10mim]Cl in the molar concentration referent to [C6mim]Cl EC50 as a function of molecular area and surface pressure.

The results for the compressibility modulus with respect to[C_4mim]Cl showed that the interactions with the monolayer described a very similar pattern to that observed for the [C_6mim][Cl]. Both ionic liquids adsorbed into the monolayer are modulating the structural properties of the film, causing the decrease of the monolayer elasticity. We observed that the incorporation of ionic liquids on the films caused changes in the maximum value of film elasticity, from 300 mN.m^{-1} for the pure DPPC film on ultra-pure water to 273 and 232 mN.m^{-1} for films containing[C_4mim]Cl and [C_6mim]Cl respectively. On the other hand, for the DPPC monolayers in the presence of [C_8mim]Cl and [C_{10}mim]Cl, the region of nearly zero elasticity, characteristic of the G phase and LE-LC phase were extinct. On these cases, the monolayers also registered a shift of the maximum compressibility modulus to lower surface pressures and a reduction in the maximum elasticity for values of 171 and 126mN.m^{-1}, respectively. These results indicate that the incorporation of long alkyl chains induces the formation of more rigid monolayers, which support the hypothesis of important implications for the stability of real cell membranes.

3.9 - Kinetics of adsorption – Ionic liquids surface activity

As stated above, the effects that might result from the interaction of the ionic liquids and cells are a consequence of their ability to approach and adsorb upon the cell membrane. We believe that for the ionic liquids that we are studying, this ability is especially important and determinant for their mechanism of action as, in many cases, they possess a significant affinity to organic phases. In order to understand the relationship between the structural aspects of the ionic liquids and their ability to interact with the cell membranes, we believe that is essential to understand the properties of the individual components intervenient and responsible to produce the phenomenon observed so far. Thus, we studied the qualitative relationship between the alkyl chain length and the surface activity of the ILs as a tool to evaluate their adsorption upon the membranes. In order to understand when and how the ionic liquid is adsorbed into the lipid monolayer, the migration from the bulk and adsorption of different ionic liquids at the air-water interface in the absence and presence of DPPC monolayers was tested. For that purpose, we monitored the variation of the water surface pressure in the presence of the ionic liquid over time. Figure 32 shows the kinetics of adsorption of [C_6mim]Cl at the air-water interface in the absence of DPPC monolayer.

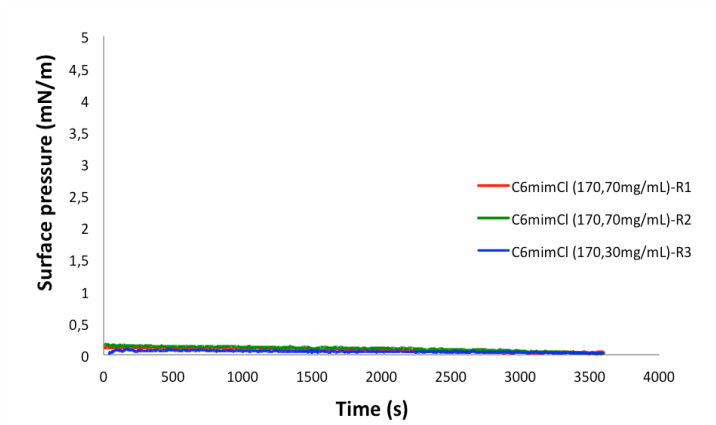

Figure 32: Kinetics adsorption of [C_6mim][Cl at the interface of the water in a concentration of 170,0 mg/L in the absence of DPPC monolayers on the surface.

From the analysis of the Figure 32 it is possible to observe that in the absence of DPPC films on the water surface (concentration at around 170 mg/L), [C_6mim]Cl showed no interfacial activity. In addition we concluded that [C_6mim]Cl is not capable of forming Langmuir or Gibbs monolayers (soluble monolayers), which is proved by the negligible alteration of the surface pressure during compression of the barriers of the Langmuir

trough (Figure 33). Notice should however be made that to comply with the software requirements of the trough to plot a π versus Area isotherm data regarding the concentration of molecules spread on the surface must be provided. Thus, in view of the fact that we do not have that information, the data entered correspond to those of DPPC. Therefore, this isotherm does not have any physical meaning.

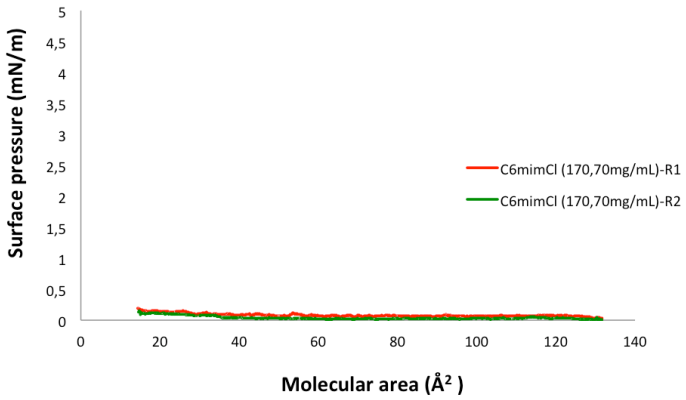

Figure 33: Pressure-area isotherms obtained by sweeping the interface of a subphase containing [C_6mim]Cl in a concentration of 170mg/L after 1hour of equilibrium and in the absence of DPPC monolayers.

Nevertheless it seems to suggest that the adsorption of [C_6mim]$^+$ to the interface might be triggered by the presence of the DPPC monolayers at the surface, in mechanisms involving electrostatic interactions between [C_6mim]$^+$ and the charged groups of the phospholipid.

Figure 34 shows the kinetics of adsorption of [C_8mim]Cl the air-water interface in the absence of DPPC monolayer.

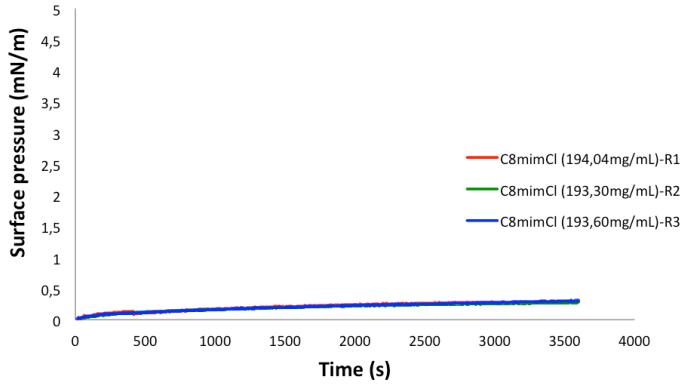

Figure 34: Kinetics adsorption of [C_8mim]Cl at the interface of the ultra-pure water (193,0 mg/L).

By the analysis of the Figure 34 we concluded that $[C_8mim]^+$ has a low surface activity. However, contrarily to $[C_6mim]^+$, the octyl alkyl chain shows some ability to form a Gibbs monolayer, as the surface pressure increased during the sweeping of the interface (Figure 35). Yet, as mentioned before, care should be taken regarding the absence of physical meaning of this plot.

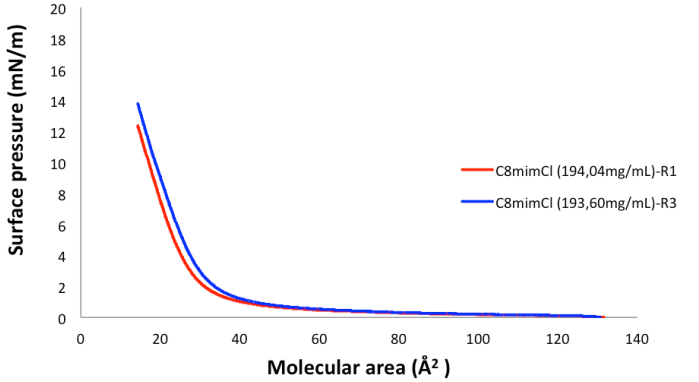

Figure 35: Pressure-area isotherms obtained by sweeping the interface of a subphase containing $[C_8mim]Cl$ in a concentration of 195mg/L after 1hour of equilibrium and in the absence of DPPC monolayers.

Nevertheless, in view of the profile of the plot shown in Fig 33 we propose that the hydration of the octyl alkyl chain of the $[C_8mim]^+$ causes an unfavorable distortion of the intermolecular structure of the water which increases the overall free energy of the system. Thus, in order to regain that entropy, the system "forces" the migration of $[C_8mim]^+$ from the subphase to the interface and the release of the associated water molecules. We suggest that at equilibrium, the $[C_8mim]^+$ will form several Gibbs monolayers distributed parallel to each other at the subphase. Each molecule from the first layer provides a spot for the molecules of the subsequent layer. The molecules following the second layer will on other hand behave as a saturated phase and migrate to upper layers only when the first and second layer experience losses of molecules (Figure 36)

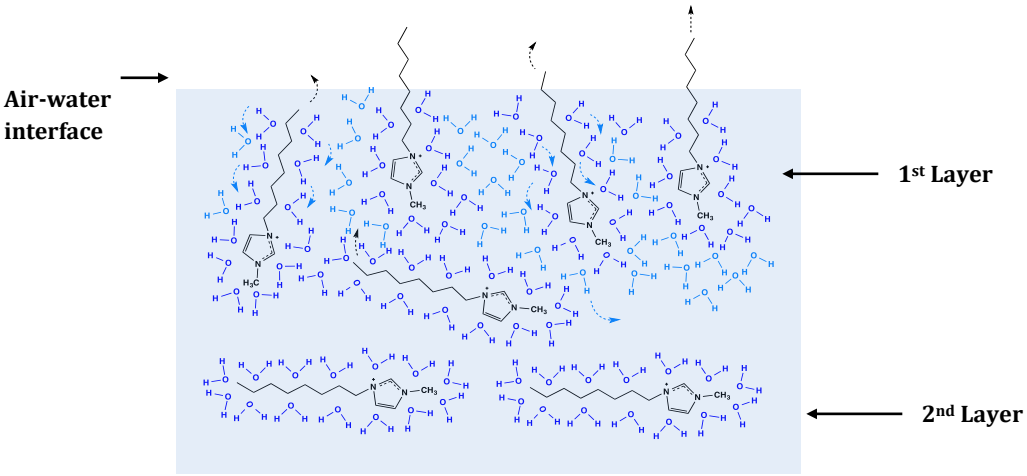

Figure 36: Representation of the $[C_8mim]^+$ migration from the bulk to the air water interface as a consequence of the low solubility of the octyl alkyl chain in water.

Figure 37 shows that, after compressing the $[C_8mim]^+$ film formed at the interface, the monolayer assumes a stable conformation at the surface. Notice that the decrease of the pressure right after the compression might be a result of the migration of $[C_8mim]^+$ molecules to the subphase due to the reduction of the free surface area available to the molecules packing, which means that the monolayers are still partially soluble in water.

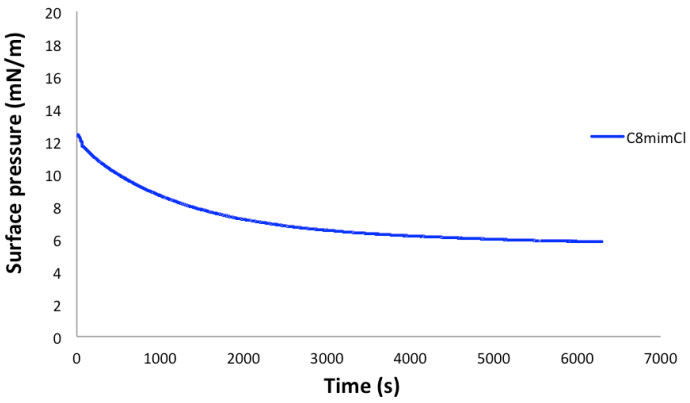

Figure 37: Stability of $[C_8mim]Cl$ monolayer formed at the interface of the water after being compressed to the minimal available surface area.

Following the same strategy we next studied the kinetic adsorption of $[C_{10}mim]Cl$ at the air-water interface in the absence of DPPC monolayers (Figure 38).

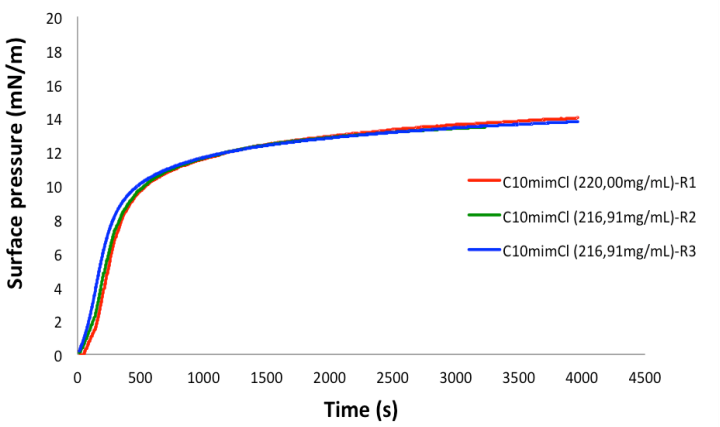

Figure 38: Kinetics adsorption of the $[C_{10}mim]^+$atthe interface of the water in a concentration of 220,0 mg/L approximately and in the absence of DPPC monolayers onthe surface.

As it is possible to observe, $[C_{10}mim]^+$ has a higher surface activity. Contrarily to $[C_8mim]^+$, the adsorption of $[C_{10}mim]^+$on the interface is significant and takes place in a really short period of time (from 0 mN/m to11 mN/min approximately 9 minutes). Upon compression of the barriers, it was possible to confirm that at the concentration of 220 $mg.L^{-1}$, the $[C_{10}mim]^+$ was able to form a monolayer at the interface (Figures 39).

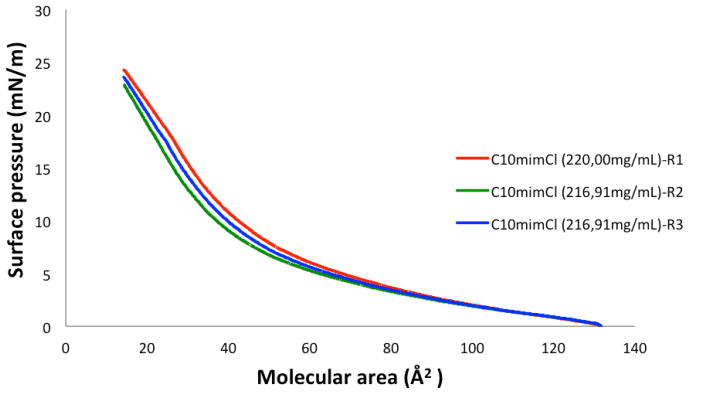

Figure 39: Pressure-area isotherms obtained by sweeping the interface of a subphase with $[C_{10}mim]Cl$ in a concentration of 193,0mg/L, after 1hour of equilibrium.

As referred before, despite of the fact that such plots lack physical meaning, these results shoe that the $[C_{10}mim]^+$ molecules adsorbed at the interface might have their alkyl chains oriented away from the subphase, which allow the formation of Langmuir monolayers. In addition, we propose that similarly to the $[C_8mim]^+$ the $[C_{10}mim]^+$ molecules are forced to move again to the bulk as a consequence of the compression of the monolayer to the minimal area available between the barriers (Figure 40)

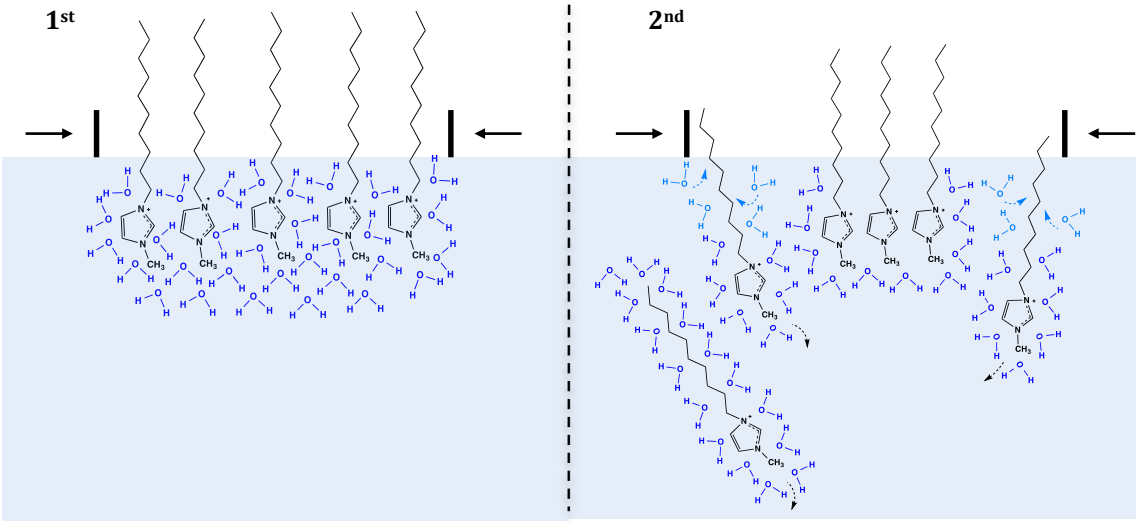

Figure 40: Migration of $[C_{10}mim]^+$ molecules from the air-water interface to the bulk as a consequence of the compression of the monolayer formed at the water surface.

Similar to what was done with $[C_6mim]Cl$ and $[C_8mim]Cl$ the stability of the compressed film was assessed. See Figure 41. As before we bealive that the surface pressure drop registered in the early stages may be due to dissolution of some $[C_{10}mim]^+$ molecules, as a result of reduced free surface area available that show the decrease of the surface pressure over time after compression. Despite of their longer alkyl chain $[C_{10}mim]^+$ doesn't seem to be able to pack efficiently enough thus some molecules are forced to migrate back into the subphase.

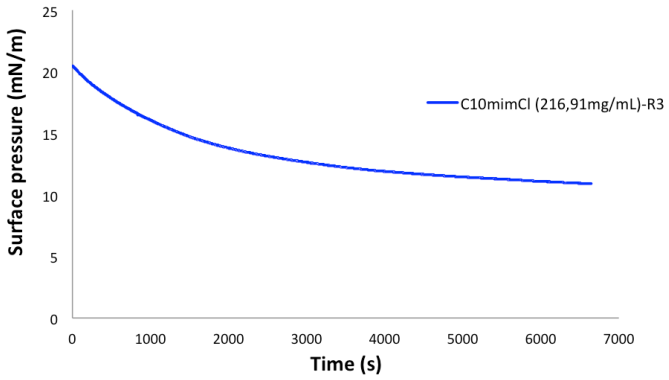

Figure 41: Study of the stability of the $[C_{10}mim][Cl]$ monolayer formed at the interface of the water.

Next the adsorption of $[C_6mim]Cl$, $[C_8mim]Cl$ and $[C_{10}mim]Cl$ in the presence of a monolayer of DPPC was studied. Figure 42 shows the kinetics of adsorption of $[C_6mim]Cl$ onto a DPPC monolayer previously compressed at a surface pressure of 16 $mN.m^{-1}$.

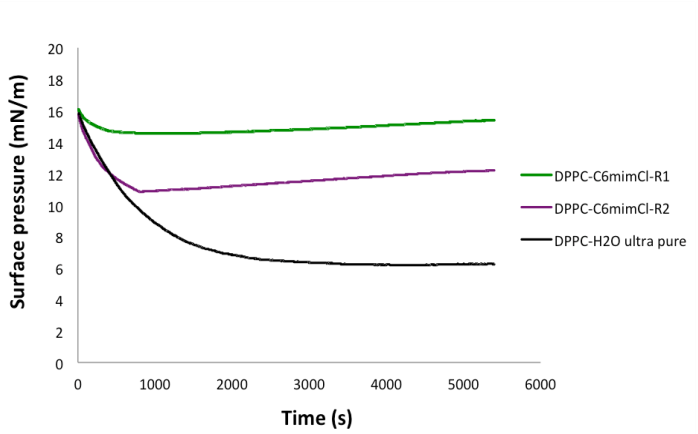

Figure 42: Kinetics adsorption of the $[C_6mim]^+$ontoDPPC Langmuir films. The concentration of the $[C_6mim][Cl]$ was 170,0 mg/L approximately.

From the analysis of the Figure 50 we were able to observe that after compressing the DPPC monolayer to a target pressure of 16 $mN.m^{-1}$, in presence and absence of the $[C_6mim]^+$ in the subphase, the surface pressure decreases. The DPPC monolayer in absence of ionic liquid in the subphase, presented a reduction of the surface pressure to 5,0 $mN.m^{-1}$. On other hand the replicate 1 and 2 presented both a reduction in the surface pressure of 15 and 11$mN.m^{-1}$ approximately. The results suggest that pure DPPC monolayers film suffered significant rearrangements along time, and that in presence of the $[C_6mim]^+$ on the subphase these rearrangements are significantly reduced. Thus, we confirmed that $[C_6mim]^+$ is able to adsorb to the DPPC monolayers, interact and cause changes in its equilibrium surface pressure. In the present test we also observed significant differences between replicates (R1 and R2), which might be due to the nature of the adsorption of the $[C_6mim]^+$. We propose that the adsorption of the $[C_6mim]^+$ might be diffusion dependent and that may be due to the fact that their approach to the DPPC monolayers will depend of their distribution on the subphase. DPPC monolayer in the presence of $[C_8mim]Cl$ and $[C_{10}mim]Cl$ in the subphase showed also lower level of rearrangements over time (Figure 43 and 44).

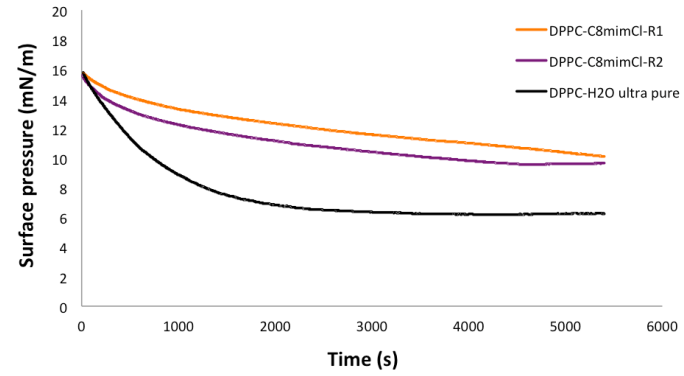

Figure 43: Kinetic of adsorption of the $[C_8mim]^+$onto DPPC Langmuir films. The concentration of the $[C_8mim][Cl]$ was 194,0mg/L approximately.

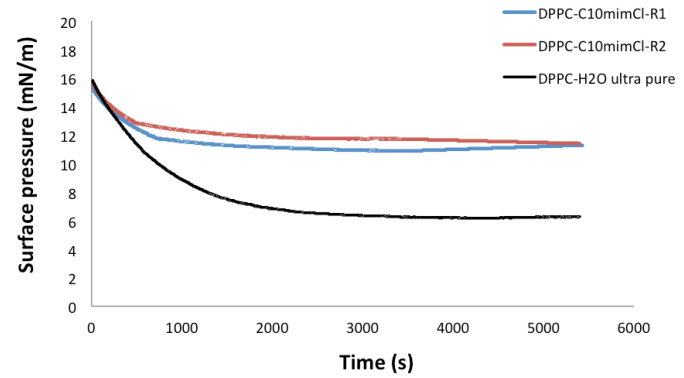

Figure 44: Kinetic of adsorption of the $[C_{10}mim]^+$onto DPPC Langmuir films. The concentration of the $[C_{10}mim]^+$ was 219,1 mg/L approximately.

Although the equilibrium surface pressure of DPPC monolayers for both $[C_8mim]Cl$ and $[C_{10}mim]Cl$ over time reaches similar values of surface pressure (around 11 ± 1mN.m^{-1}), monolayers in presence of $[C_{10}mim]Cl$ achieved the equilibrium in shorter periods of time than monolayers in presence of $[C_8mim]Cl$. These results were expected because, as discussed before, the adsorption of $[C_{10}mim]^+$ on the interface is significant and takes place in a really short period of time. Notice that the replicates of both ILs had higher similarities than those obtained for assays with $[C_6mim]Cl$. The results suggest that with the increase of the alkyl chain the ILs will adsorb more to the DPPC monolayer, and that contrary to ILs of short alkyl chain, the adsorption will not be dependent of diffusion phenomena.

3.9.1 - Kinetics adsorption of [C_6mim]Cl, [C_8mim]Cl and [C_{10}mim]Cl by injection into the subphase

The injection of the specific molecule in the subphase is an important methodology on the evaluation of the modification caused by the insertion of molecules of a second component in superficial monolayers. A typical injection experiment might involve the formation of an insoluble monolayer at a specific surface pressure, after which a soluble surface material is injected below the film. The changes in surface pressure (at constant area) induced by the adsorption or penetration of the new material in the monolayer are monitored and used to study the new properties of the mixed films formed (Figure 45).

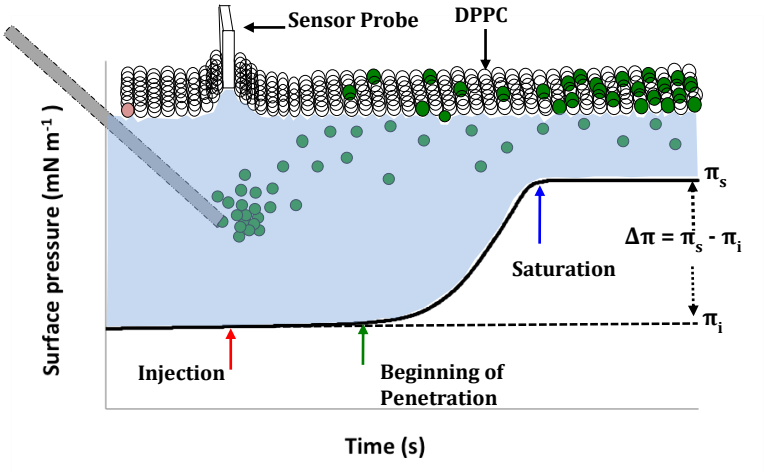

Figure 45: Kinetic of the rearrangements suffered by a DPPC Langmuir monolayer along time after compression until the target pressure and injection of a specific molecule.

Considering this approach, DPPC monolayers were compressed up to a surface pressure of 16mN.m^{-1}, the area between the barriers was then fixed and the surface pressure was recorded over time. When the surface pressure was stabilized, 1 mL of an IL solution (concentration similar to the [C_6mim]Cl EC_{50} value) was injected in the subphase and the changes in the surface pressure monitored and considered for further discussion. At the pressure of 16 mN.m^{-1} the monolayer is at the beginning of the LC phase, which ensure the formation of DPPC domains according to typical morphology, guarantee a high level of organization and allow the evaluation of the penetration ability of the ILs.

Figure 46 shows the relaxation behavior of a DPPC monolayer on ultrapure water under constant area and upon compression up to 16mN.m^{-1}. The relaxation curve is represented by the ratio of the surface pressure variation of the DPPC monolayer with time.

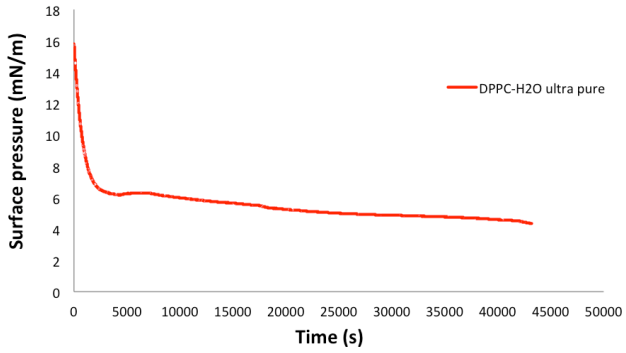

Figure 46: Kinetics of the rearrangements suffered by a DPPC Langmuir monolayer during 12 hours after compression at 16 mN/m.

From a general analysis of the relaxation behavior, it is possible to observe that the surface relaxation of DPPC monolayer suffered a significant drop. As at the surface of ultra-pure water the DPPC monolayer has no net charge (zwitterion), the repulsive forces between molecules should not be significant thus, higher levels of stability than those obtained by us would have been expected. Yet, this film exhibited a 37% reduction of the surface pressure after approximately 5 hours of relaxation. This abrupt change in the surface pressure stability suggests that the monolayer suffers rearrangements of the molecular structure, reorientation of the phospholipids alkyl chains or loss of material along time. As at the surface pressure of 16mN/m, the interaction between the molecules of the DPPC monolayer might depend on the molecular area, small morphological changes resulting from the relaxation of the DPPC monolayer seem to induce significant changes of the surface pressure.

Figure 47 shows the adsorption kinetics of $[C_6mim]Cl$ on a DPPC monolayer after injection of a solution with a concentration of 170 $mg.L^{-1}$.

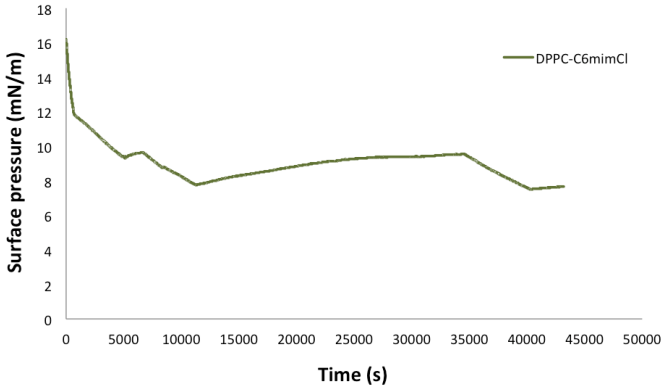

Figure 47: Kinetics of rearrangements suffered by a DPPC Langmuir monolayer after compression to the target pressure of 16 mN/m and injection of a solution of $[C_6mim]Cl$ in the subphase.

After the compression of the DPPC monolayer up to 16mN.m^{-1}, the monolayer was allowed to stabilize (i.e. permitting the molecules to adopt the most stable morphological conformation) and then an IL solution was injected. As shown in Figure 42, it is possible to observe that the surface pressure only suffers a small variation over time, which could be related with the adsorption of [C_6mim]Cl into the monolayer.

This experiment was then performed using a higher concentration of IL. Figure 48 shows the adsorption kinetic of the [C_8mim]Cl onto a DPPC monolayer after injection of a solution with a concentration of 195 mg.L^{-1}, which is equivalent to the molar concentration of the [C_6mim]Cl EC_{50}.

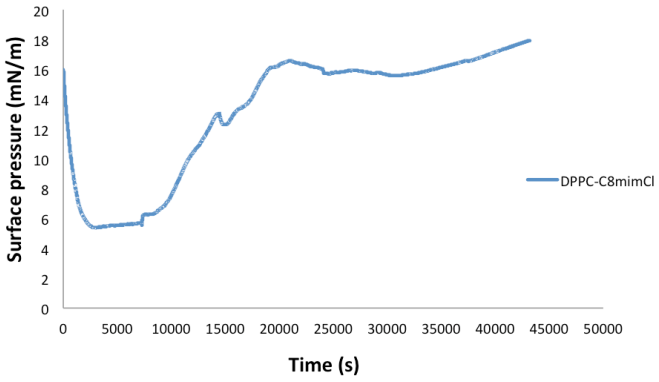

Figure 48: Kinetics of rearrangements suffered by a DPPC Langmuir monolayer after compression at the target pressure of 16 mN/m and injection of a solution of C_8mimCl in the subphase.

The injection of the [C_8mim]Cl in the subphase induced the increase of the surface pressure. Thus, we conclude that the[C_8mim]$^+$ adsorbed and penetrated the film. As there are several points at which the curve shows the increase and after a decrease of the surface pressure, we propose that the rearrangements of the monolayer induces the exclusion of [C_8mim]$^+$ which is later re-adsorbed.

Figure 49 shows the adsorption kinetic of the [C_{10}mim]Cl onto a DPPC monolayer after injection of a solution with a concentration of 220 mg.L^{-1}, which is equivalent to the molar concentration of the [C_6mim]Cl EC_{50}.

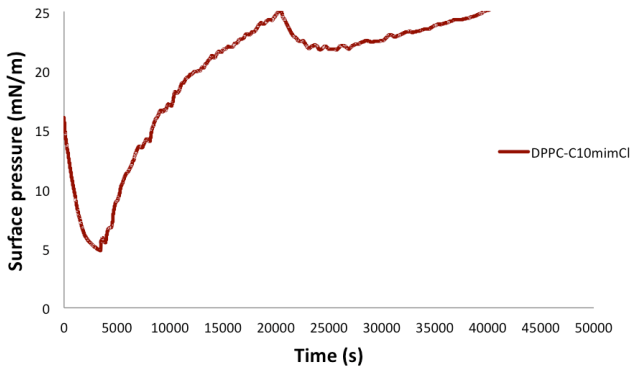

Figure 49: Kinetics of rearrangements suffered by a DPPC Langmuir monolayer after compression at the target pressure of 16 mN/m and injection of a solution of C_{10}mimCl in the subphase.

As expected, the kinetics of adsorption of [C_{10}mim]Cl on the DPPC monolayer showed the highest effect on the surface pressure. After injection, the monolayer suffered a faster variation of the surface pressure when compared with the remaining ionic liquids. At the surface pressure of 25mN.m^{-1} an abrupt decrease was observed. After this decrease, the [C_{10}mim]Cl starts to be adsorb again and penetrate into the monolayer. At the end of the experiment neither [C_8mim]Cl nor [C_{10}mim]Cl have reached the surface pressure equilibrium. Therefore, the results obtained indicate that, the adsorption and penetration as well as the orientation of the phospholipids alkyl chains proceeds over a very long period of time. Although not tested in this work, future studies should take in consideration the evaluation of the ILs penetration on DPPC monolayers at pressures as 0 and 35 mN.m^{-1}. These additional studies will provide the opportunity to understand in more detail the ability of the penetration ability of the IL's tested here.

4–Mechanism of interaction between [$C_n$mim]Cl and DPPC monolayers

Many of the natural phenomena concerning biological assemblies such as those involving the cell membrane are a result of physical, intra- and intermolecular interactions. These forces operate between the macromolecules by nonspecific, nonstoichiometric and strongly directional forces over distances greater than those of covalent bonds. They are therefore the electrostatic and hydrophobic interactions, the hydrogen bonds and the van der Waals forces. Due to the structural versatility and complexity of the ionic liquid and the phospholipids used on this work it is more than expected the contribution of different types of forces during the intermolecular interactions of both molecules. In the last years studies using the Langmuir Blodgett technique have been pointing fundamental forces as electrostatic and more recently hydrophobic interactions as the trigger forces of complex interactions involving cellular membranes and specific macromolecules. As it is know, the electrostatic interactions between charged atoms or molecules arise when two or more molecules or atoms, with identical or opposite charge, approach and interacts with each other. Considering the zwitterion nature of DPPC phospholipid, the electrostatic interactions between the charged moieties and the ionic liquids will assume the form of repulsive or attractive forces depending of both the distance between the charges and nature of the intervening medium. The capability of both phosphate and glycerol moieties of DPPC phospholipids to establish strong hydrogen bonding with water molecules, make the negatively charged group surrounded by water molecules **(Ma G. and Allen H.C., 2006)**. The hydrogen-bonding network between water molecules and the phosphate moiety as well as the distribution of the negative charge between the four oxygen atoms, lower the spatial electronic density and weakens the PO_2^-group **(Shapovalov V. L., 1998; Ma G. and Allen H.C., 2006)**. Thus, the solvation of the phosphate group by interfacial water might hinder the approach or the electronic interaction of hydrophobic charged molecules **(Shapovalov V. L., 1998)**. As the ammonium group possesses a more free motion compared to the phosphate moiety, which is linked to the glycerol and choline group, the positive moiety will have a much higher sensitivity to the presence of charged molecules in the head group vicinity. The incapability of the ammonium group to establish hydrogen bonds and the presence of the positive charge on a single nitrogen atom highly favors electrostatic interactions with hydrophobic ILs **(Shapovalov V. L., 1998)**.

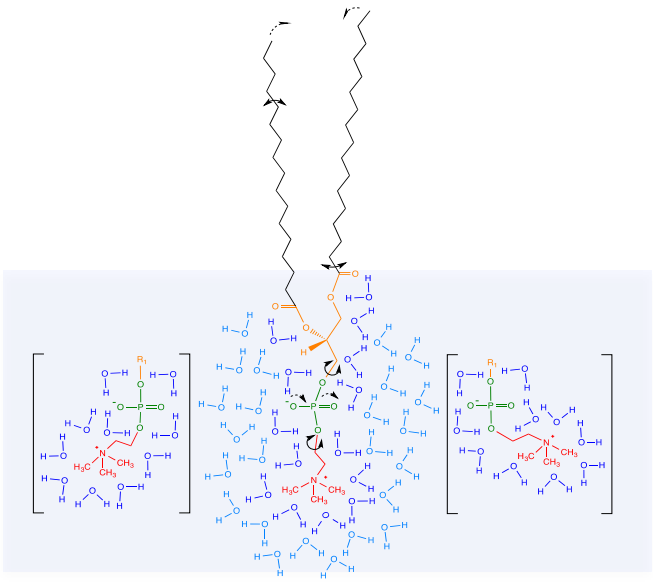

Figure 50: Representation of the DPPC phospholipids polar head hydration and illustration of the motion of the ammonium moiety in a 2D plane.

According to that, we propose that both the approach and establishment of electrostatic interactions between the $[C_6mim]^+$ and the DPPC head group might be more favorable via the positively charged ammonium group than with the negative phosphate moiety. If this scenario was to happen, strong long-range electrostatic repulsions will take place between the positively ammonium groups and the cation $[C_6mim]^+$. Hence, We propose that initially, when the DPPC monolayer is starting to organize, these repulsive interactions favor and induce the formation of DPPC LE phase domains. Moreover, these repulsion forces and the hydration state of the phosphate group prevent the $[C_6mim]^+$ of penetrating the film, allowing the transition of the lipidic domains from LE to the LC morphology to occur normally. At the beginning of the LC phase, the area around each DPPC molecule reaches a minimum stage, making the water of the hydration shell to be squeezed out. Then, the less hydrated state of the phosphate group strengthens PO_2^-, allowing the $[C_6mim]^+$ to surpass the repulsion forces with the ammonium group and be attracted by the negatively charged phosphate moiety. With that, the $[C_6mim]^+$ is able to incorporate into the head group region, establishing strong local binding involving electrostatic attraction and induce the expansion of head groups of the neighbour phospholipids (steric effect). Finally, the low solubility of the alkyl chain of the $[C_6mim]^+$in water induces its penetration into the DPPC monolayer, allowing the establishment of hydrophobic and van der Waals interactions with the aliphatic chain of the DPPC molecules. As a consequence of the establishment of these interactions, the $[C_6mim]^+$ is not expelled from the monolayer at high pressures and the monolayer remains expanded. As

the concentration of the [C_6mim]Cl increases, the interaction level and binding with the DPPC monolayer is enhanced and the expansion effect is increased (Figure 51).

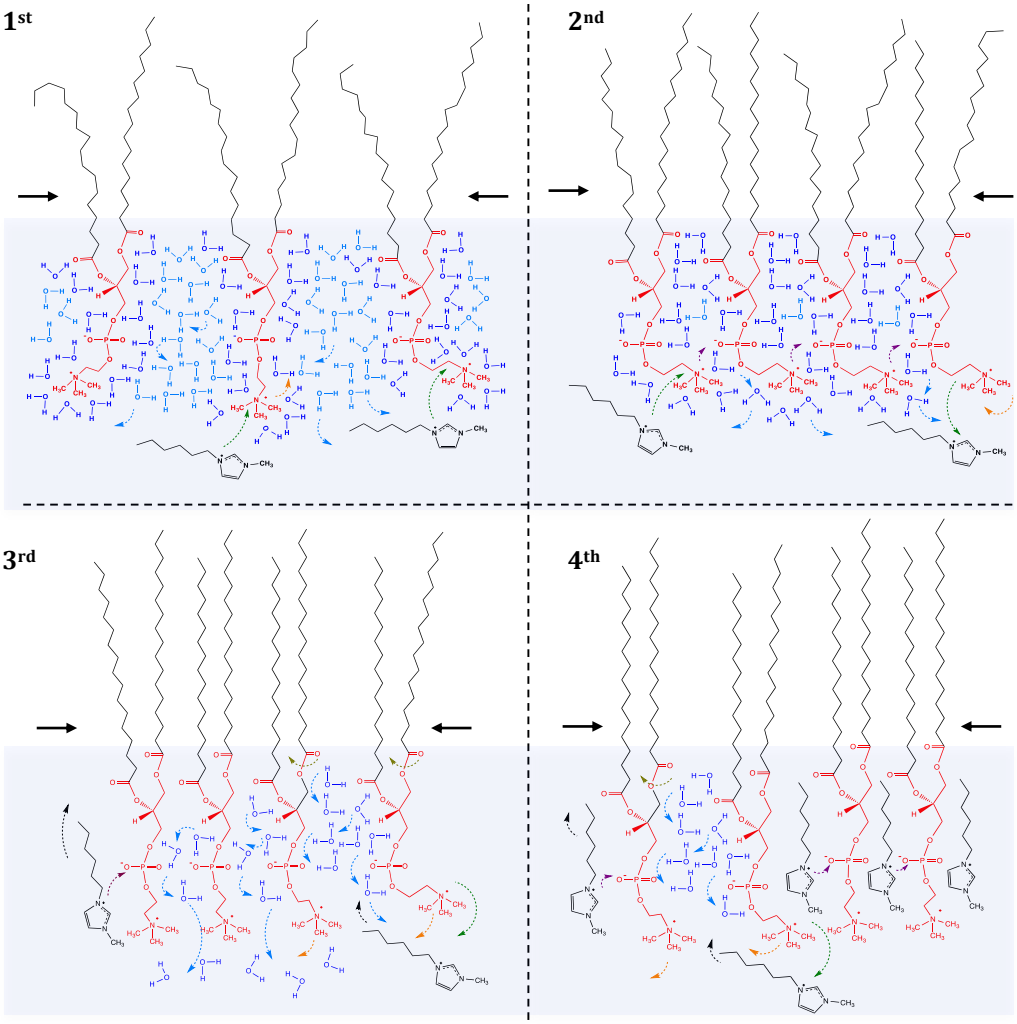

Figure 51: Representation of a possible mechanism of interaction between [C_6mim]Cl and DPPC monolayers taking in consideration the results obtained and discussed before.

The ability to form hydrogen bonds as well as the absence of the nonpolar moiety suggest that comparatively to the [C_6mim]$^+$ it would be easier for the [Chol]$^+$ to incorporate the polar faction of the DPPC monolayer. However, our results show that similarly to [C_6mim]Cl, [Chol]Cl only induces changes on DPPC monolayers at higher levels of packing. We suggest that similarly to the [C_6mim]Cl, the phosphate moiety hydration state affects the interactions between the [Chol]$^+$ and the DPPC head group. This effect might be once more due to the inability of the cation to be attracted with enough strength by the negative moiety and surpass the electrostatic repulsions with the ammonium group.

Thus, we propose that at beginning of the compression the $[Chol]^+$ interacts with the DPPC monolayer manly by electrostatic repulsion. At higher levels of organization the $[Chol]^+$ surpasses the electrostatic repulsions, and penetrates into the head group of the DPPC monolayer establishing strong local electrostatic attractions with the negative phosphate group causing the expansion of the monolayer. At high surface pressure the $[Chol]^+$ is then expelled from the DPPC monolayer to the subphase and the monolayer adopts a compact morphology (Figure 52).

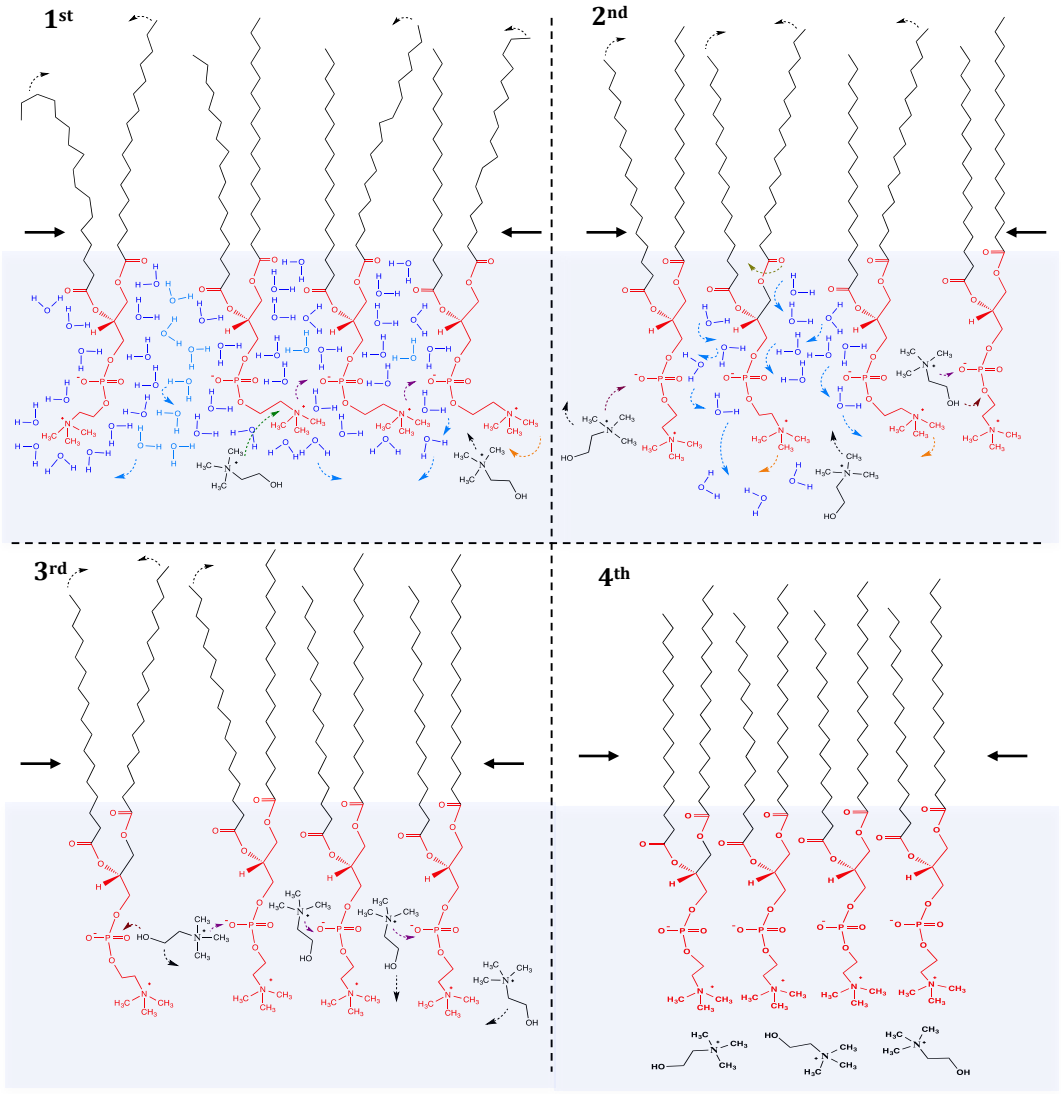

Figure 52: Representation of a possible mechanism of interaction between [Chol]Cl and DPPC monolayers taking in consideration the results obtained and discussed before.

The ejection of the [Chol]+ from the monolayer at higher pressures, supports the importance of the hydrophobic/lipophilic character of ILs cations in the interactions with lipidic monolayers. Thus we propose that $[C_8mim]^+$ mechanism of interaction with the

DPPC monolayers will comprise a stronger contribution of hydrophobic interactions but also a contribution of electrostatic interaction as for the $[C_6mim]^+$. In what concerns the interactions between $[C_{10}mim]^+$ and DPPC monolayers, we concluded that during the adsorption of molecules to the interface the alkyl chain will be preferably orientated in the plan at which the unfavourable interactions between the aqueous phase and the nonpolar sections are minimal. The resulting molecular orientation will induce the spontaneous penetration of the alkyl chain in the DPPC monolayer. Thus, the alkyl chain of the ionic liquids will interact with the lipidic monolayers through hydrophobic interactions, the monolayer will be expanded and the arrangement of the DPPC molecules will be affected (Figure 53)

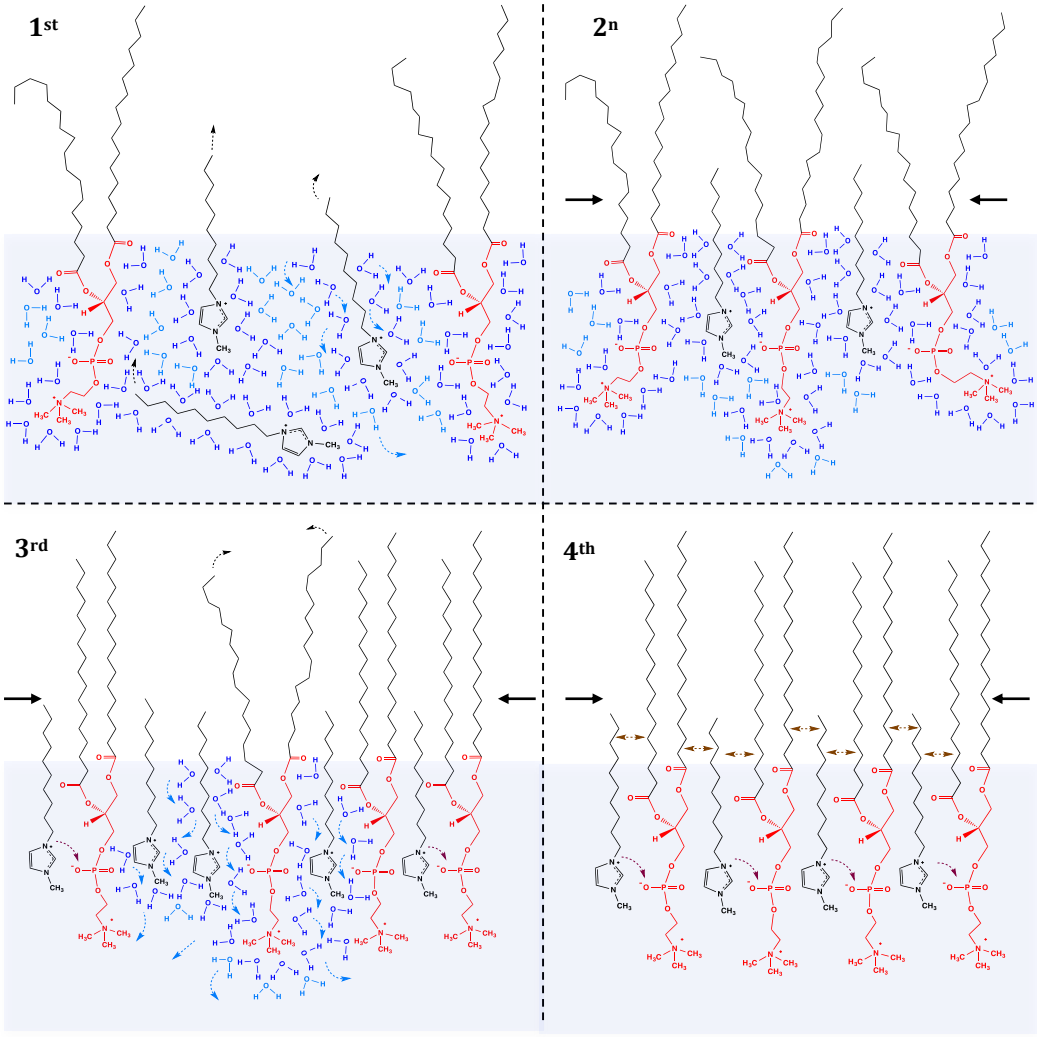

Figure 53: Representation of a possible mechanism of interaction between $[C_{10}mim]Cl$ and DPPC monolayers taking in consideration the results obtained and discussed before.

4 – Conclusions and Future Work

Based in our results we concluded that the interaction and adsorption of ionic liquids on the DPPC monolayer were manly dependent of the alkyl chain length, and that the effects were higher for [C_{10}mim]Cl than for [C_6mim]Cl. Through the adsorption kinetics, we concluded that the [C_6mim]Cl is not surface active but that its adsorption was triggered by electrostatic interaction with the lipidic monolayers and that the interactions involving the [C_8mim]Cl and [C_{10}mim]Cl were ruled manly by their hydrophobic/lipophilic character. We also concluded that contrary to the [Chol][Cl], the effects of [C_6mim][Cl] depend on the concentration, which suggests that the mechanism of action of both ILs families is different. It is possible to conclude by our results that imidazolium ILs will have their ability to expand and remain on the monolayer decreased with the decrease of their alkyl chain length and that short lateral chains (C2 and C4) will only adsorb reversely on the phospholipid monolayer while long chains (C8 and C10) will adsorb irreversibly and promote stronger interactions. The observation of more drastic rearrangements, such as the removal, loss and dissolution of lipid molecules, was not observed throughout our studies.

In order to obtain a deeper understanding of the phenomena occurring during the interactions between the ILs and the DPPC monolayers and validate the mechanism of interaction here proposed additional studies are required. These studies might consider an evaluation of the stage of nucleation and growth of phospholipid domains of DPPC monolayers in presence of ionic liquids as well as the evaluation of the ionization state of DPPC monolayer during the compression. For that, we recommend for example the combination of two analysis: a) Brewster Angle Microscopy analysis, which will allow direct observations of the kinetics of the nucleation process on the DPPC monolayer; b) Surface potential measurements, which will allow us to evaluate the orientation of specific dipoles of the DPPC monolayer and finally c) sum-frequency generation (SFG) spectroscopies to evaluate the type of functional groups and their orientation at the interface.

6 - Bibliography

Anastas P., Eghbali, N. (2010). *Chemical Society Reviews*, *39*, 301.

Antonietti M., Kuang, D., Smarsly, B., and Zhou, Y. (2004).*Angewandte Chemie International Edition,* 43, 4988.

Aroti, A., E. Leontidis, E. Maltseva, and G. Brezesinski. (2004). *Journal of Physical Chemistry B*. 108, 15238-15245.

Bernot R. J., Brueseke, M. A., Evans-White, M. A., Lamberti, G. A. (2005). *Environmental Toxicology and Chemistry*, *24*, 87.

Bourbigou O., H., Magna L., (2002).*Journal of Molecular Catalysis A: Chemical,* 182, 419.

Brennecke J. F., Maginn, E. J. (2001). *AIChE Journal*, *47*, 2384.

Brockman H. (1999). *Current opinion in structural biology*, *9*, 438.

Cancino, J., Nobre, T. M., Oliveira Jr, O. N., Machado, S. A., Zucolotto, V. (2013). *Nanotoxicology*, *7*, 61.

Cary W., and T. Kyle Vanderlick. (1997). *Langmuir*, 26. 7158-7164.

Couling D. J., Bernot, R. J., Docherty, K. M., Dixon, J. K., Maginn, E. J. (2006). *Green Chemistry*, *8*, 82.

Cocalia V.A., Gutowski, K.E., Rogers, R.D. (2006). *Coordination Chemistry Rev*iews, 250, 755.

Cho C. W., Pham, T. P. T., Jeon, Y. C., Vijayaraghavan, K., Choe, W. S., Yun, Y. S. (2007). *Chemosphere, 69*. 1003.

Clausell A., Busquets, M. A., Eeman Pujol, M., Alsina, A., Cajal, Y. (2004). *Biopolymers75*, 480.

Crawford, N. F., Leblanc, R. M. (2013). *Advances in colloid and interface science*.

J. T.Davies, E.K.Rideal, Interfacial Phenomena,Academic Press,New York,1963.

Devanathan S., Salamon, Z., Lindblom, G., Gröbner, G., Tollin, G. (2006). *FEBS Journal*, *273*, 1389.

Docherty, K. M., Kulpa Jr, C. F. (2005). *Green Chemistry*. *7*, 185.

Duncan, S. L., & Larson, R. G. (2008). *Biophysical journal*, *94*(8), 2965-2986.

Dynarowicz-Łątka, P., Dhanabalan, A., Oliveira Jr, O. N. (2001). *Advances in colloid and interface science*, *91*, 221.

Eeman M., Deleu, M. (2010). *Biotechnologie, Agronomie, Société et Environnement*, *14*, 719.

Frade R. F., Matias, A., Branco, L. C., Afonso, C. A., Duarte, C. M. (2007). *Green Chemistry*, *9*, 873.

Frade R. F., Rosatella, A. A., Marques, C. S., Branco, L. C., Kulkarni, P. S., Mateus, N. M., Duarte, C. M. (2009). *Green Chemistry*, *11*, 1660.

Freire M. G., Neves, C. M., Carvalho, P. J., Gardas, R. L., Fernandes, A. M., Marrucho, I. M., Coutinho, J. A. (2007). *The Journal of Physical Chemistry B*, *111*, 13082.

Gal N., Malferarri, D., Kolusheva, S., Galletti, P., Tagliavini, E., Jelinek, R. (2012). *Biochimica et Biophysica Acta (BBA)-Biomembranes*, 12, 2967.

Galluzzi M., Zhang, S., Mohamadi, S., Vakourov, A., Podestà, A., Nelson, A. (2013).*Langmuir*, 29, 6573.
Gathergood N., Garcia, M. T., Scammells, P. J. (2004). *Green Chemistry*, *6*, 166.
Garcia M. T., Gathergood, N., & Scammells, P. J. (2005). *Green Chemistry*, *7*, 9.
Gennis, R.B. (1989). Biomembranes: Molecular Structure and Function. *Springer-Verlag, New York*.
Guzmán, E., Liggieri, L., Santini, E., Ferrari, M., & Ravera, F. (2013).*Biointerfaces*, *105*, 284**.**
Hann, R. A., Kathirgamanathan, P. (1990). *Philosophical Transactions of the Royal Society of London.Series A, Mathematical and Physical Sciences*. *330*, 141.
Huang, Z., Zheng, X., Yan, D., Yin, G., Liao, X., Kang, Y., Hao, B. (2008). *Langmuir*, *24*, 4140.
Huddleston J., Rogers, R. (1998). *Chemical Communications*, 16, 1765.
Hansch C., Leo, A. (1979). *Substituent constants for correlation analysis in chemistry and biology* (pp. 18-43). New York: Wiley
Iwamoto M., Mizutani, Y., Sugimura, A. (1996). *Physical Review B*, *54*, 8186.
Ihalainen, P., Peltonen, J. (2003). *Langmuir*, *19*, 2226.
Jennings V. L., Rayner-Brandes, M. H., & Bird, D. J. (2001). *Water research*, *35*, 3448.
Kawai K., Kaneko, K., Kawakami, H., Yonezawa, T. (2011). *Langmuir*, *27*, 9671.
Kawai K., Kaneko, K., Kawakami, H., Narushima, T., Yonezawa, T. (2012).*Colloids and Surfaces B: Biointerfaces*, 102, 9.
Kaganer V. M., Möhwald, H., Dutta, P. (1999). *Reviews of Modern Physics*, *71*, 779.
Kessler P. D., Marchbanks, R. M. (1979). Nature, 279, 542.
Khan M. S., Dosoky, N. S., Williams, J. D. (2013).*International journal of molecular sciences.14*, 21561.
Koel M. (2005). *Critical Reviews Analytical Chem*istry, 35, 177.
Kubisa P. (2005). *Journal of Polymer Sience: Polymer Chemistry,* 43, 4675.
Kumar R. A., Papaïconomou, N., Lee, J. M., Salminen, J., Clark, D. S., Prausnitz, J. M. (2009). *Environmental toxicology*, *24*, 388.
Khattari, Z., U. Langer, S. Aliaskarisohi, A. Ray, and Th M. Fischer. (2011). *Materials Science and Engineering,* 31(8), 1711-1715.
Latała A., Stepnowski, P., Nędzi, M., Mrozik, W. (2005).*Aquatic Toxicology*, *73*, 91.
Leblanc R. M. (2006). *Current opinion in chemical biology*, *10*, 529.
Luis P., Ortiz, I., Aldaco, R., Irabien, A. (2007). *Ecotoxicology and environmental safety*, *67*, 423.
Ma, G., & Allen, H. C. (2006). *Langmuir*, *22*(12), 5341-5349.
Marsh D. (1996). *Biochimica et Biophysica Acta (BBA)-Reviews on Biomembranes*, *1286*(3), 183-223.
Matzke M., Arning, J., Ranke, J., Jastorff, B., Stolte, S. (2010). *Handbook of Green Chemistry*, 6, 233.

Matzke M., Stolte, S., Thiele, K., Juffernholz, T., Arning, J., Ranke, J., Jastorff, B. (2007).*Green Chemistry*, *9*, 1198.
Matsuzaki K. (2007). *Biochim et Biophys Acta*, 1768,1935.
Mingeot-Leclercq M. P., Deleu, M., Brasseur, R., Dufrêne, Y. F. (2008). *Nature protocols*, *3*,1654.
Notter, R. H., Tabak, S. A., Mavis, R. D. (1980). *Journal of lipid research,* 21(1), 10-22.
Notter, R.H. (2000). Lung Surfactants: basic science and clinical applications. *Marcel Dekker, New York.*
OECD 2008, Guidelines for the testing of chemicals. Test 211, *Daphnia magna* Reproduction Test.
OECD 2011, Guidelines for the testing of chemicals. Test 201, Freshwater Alga and Cyanobacteria, Growth Inhibition Test.
OECD 2006, Guidelines for the testing of chemicals. Test 221, *Lemna* sp. Growth Inhibition Test.
OECD 2004, Guidelines for the testing of chemicals. Test 202, *Daphnia* sp. Acute Immobilisation Test.
Orbulescu, J., Leblanc, R. M. (2009). *The Journal of Physical Chemistry C*, *113*, 5313.
Pavinatto, F. J., Santos Jr, D. S. D., Oliveira Jr, O. N. (2005). *Polímeros*. *15*, 91.
Pavinatto, F. J., Pacholatti, C. P., Montanha, É. A., Caseli, L., Silva, H. S., Miranda, P. B., Oliveira Jr, O. N. (2009). *Langmuir*, *25*, 10051.
Pavinatto, F. J., Caseli, L., Pavinatto, A., dos Santos, D. S., Nobre, T. M., Zaniquelli, M. E., & de Oliveira, O. N. (2007). *Langmuir*, *23*(14), 7666-7671.
Parra-Barraza, H., Burboa, M. G., Sánchez-Vázquez, M., Juárez, J., Goycoolea, F.M., Valdez, M. A. (2005). *Biomacromolecules*, *6*, 2416**.**
Peric B., Marti, E., Sierra, J., Cruañas Terradas, R., Garau, M. A. (2012). *Recent Advances in Pharmaceutical Sciences II, 89, 113*
Petty, M. C. (1996). *Langmuir-Blodgett films: an introduction*. Cambridge University Press.
Peetla C., Stine, A., Labhasetwar, V. (2009).*Molecular pharmaceutics*, *6*, 1264.
Pham T. P. T., Cho, C.-W., Yun, Y.-S., 2009. *Water Research,* 44, 352.
Plechkova, N. V., Seddon, K. R. (2008). *Chemical Society Reviews*, *37*, 123.
Prasad, A. K., Kumar, V., Malhotra, S., Ravikumar, V. T., Sanghvi, Y. S., Parmar, V. S. (2005). *Bioorganic & medicinal chemistry*, *13*, 4467.
Pretti C., Chiappe, C., Pieraccini, D., Gregori, M., Abramo, F., Monni, G., Intorre, L. (2006). *Green Chemistry*, *8*, 238.
Pretti C., Chiappe, C., Baldetti, I., Brunini, S., Monni, G., Intorre, L. (2009).*Ecotoxicology and environmental safety*, *72*, 1170.
Planque M. R., Raussens, V., Contera, S. A., Rijkers, D. T., Liskamp, R. M., Ruysschaert, J. M., Watts, A. (2007). *Journal of molecular biology*, *368*, 982.
Paun G., Rozenberg, G. (2002). *Theoretical Computer Science*, *287*, 73.

Ranke J., Mölter, K., Stock, F., Bottin-Weber, U., Poczobutt, J., Hoffmann, J., Jastorff, B. (2004). *Ecotoxicology and Environmental Safety*, *58*, 396.
Ranke J., (2007). *Green Chemistry*, *9*, 760.
Regulation E. C. (1999). No 1907/2006 of the European Parliament and of the Council of 18 December 2006, concerning the Registration. *Evaluation, Authorization and Restriction of Chemicals (REACH)*.
Schwartz D. K. (1997). *Surface Science Reports*, *27*, 245.
Seddon K. R. (1997). *Journal of Chemical Technology and Biotechnology*, *68*, 351**.**
Shapovalov, V.L. (1998). *Thin Solid Films*.327, 599-602.
Silva, C. A., Nobre, T. M., Pavinatto, F. J., Oliveira Jr, O. N. (2012). *Journal of colloid and interface science*, *376*, 289.
Singer S. J., Nicolson, G. L. (1972). *Science*, *175*, 720.
Sikkema J., De Bont, J. A., Poolman, B. (1995). *Microbiological reviews*, *59*, 201
Singer S. J., Nicolson, G. L. (1972). *Science*, *175*, 720.
Stolte S., Arning, J., Bottin-Weber, U., Matzke, M., Stock, F., Thiele, K., Ranke, J. (2006).*Green Chemistry*, *8*, 621.
Stepnowski P., Zaleska, A. (2005). *Journal of Photochemistry and Photobiology A: Chemistry*, *170*, 45.
Steinberg S. M., Poziomek, E. J., Engelmann, W. H., Rogers, K. R. (1995). *Chemosphere*, *30*, 2155.
Sung C. P., Johnstone, R. M. (1965). *Canadian Journal of Biochemistry*, *43*, 1111.
Schmidt, T. F., Caseli, L., Nobre, T. M., Zaniquelli, M. E., & Oliveira Jr, O. N. (2008). *Colloids and Surfaces A: Physicochemical and Engineering Aspects*, *321*(1), 206-210.
Sheldon R. (2001). *Chemical Communications*, 23, 2399.
Tabak, S.A., R.H. Notter, J.S. Ultman, and S.M. Dinh. (1977). *Journal of Colloid and Interface Science*, 60, 117-125.
Tabak, S.A., and R.H. Notter. (1977). *Review of Scientific Instruments*.48, 1196-1201.
Torrano A. A., Pereira, Â. S., Oliveira Jr, O. N., Barros-Timmons, A. (2013). *Colloids and Surfaces B: Biointerfaces*, 108,120.
Thakur G., Micic, M., Leblanc, R. M. (2009). *Colloids and Surfaces B: Biointerfaces*, *74*, 436.
Ventura S. P., Gardas, R. L., Goncalves, F., Coutinho, J. A. (2011). *Journal of Chemical Technology and Biotechnology*, *86*, 957.
Ventura S. P., Marques, C. S., Rosatella, A. A., Afonso, C. A., Goncalves, F., Coutinho, J. A. (2012-a). *Ecotoxicology and environmental safety*, *76*, 162.
Ventura S. P., de Barros, R. L., Sintra, T., Soares, C. M., Lima, A. S., & Coutinho, J. A. (2012-b). *Ecotoxicology and environmental safety*, 83, 55.
Ventura S. P., Gonçalves, A. M., Sintra, T., Pereira, J. L., Gonçalves, F., Coutinho, J. A. (2013). *Ecotoxicology*, *22*, 1.
Verdier Y., Zarándi, M., Penke, B. (2004). *Journal of Peptide Science*. *10*, 229.

Vestergaard M. D., Hamada, T., Takagi, M. (2008).*Biotechnology and bioengineering*. *99*, 753.

Wasserscheid P., Welton, T. (2008). *Ionic liquids in synthesis* (Vol. 1). Weinheim: Wiley-Vch.

Wang, Z., & Yang, S. (2009). *ChemPhysChem*, *10*(13), 2284-2289.

Welton T. (1999). *Chemical reviews*, *99*, 2071.

Wüstneck, N., R. Wüstneck, V.B. Fainerman, U. Pison, and R. Miller. (2000). *Colloids and Surfaces A: Physicochemical and Engineering Aspects,*164, 267-278.

Zaitsev, S.Y., V.P. Vereschetin, V.P. Zubov, W. Zeiss, and D. Möbius. (1996). *Thin Solid Films*.285, 667-670.

Zhang S., Lu, X., Zhang, Y., Zhou, Q., Sun, J., Han, L. (2008). *Spinger-Verlag*. DOI:10.1007430.

Zhao D., Wu, M., Kou, Y., Min, E. (2002).*Catalysis today*, *74*(1), 157-189.